Journal Pre-proofs

Review

Curcumin encapsulation in nanostructures for cancer therapy: a 10-year overview

Natália A. D'Angelo, Mariana A. Noronha, Isabelle S. Kurnik, Mayra C. C. Câmara, Jorge Vieira, Luís Abrunhosa, Joana T. Martins, Thais F. R. Alves, Louise L. Tundisi, Janaina A. Ataide, Juliana S. R. Costa, Angela F. Jozala, Laura O. Nascimento, Priscila G. Mazzola, Marco V. Chaud, António A. Vicente, Andre M. Lopes

Please cite this article as: N.A. D'Angelo, M.A. Noronha, I.S. Kurnik, M. C. C. Câmara, J. Vieira, L. Abrunhosa, J.T. Martins, T. F. R. Alves, L.L. Tundisi, J.A. Ataide, J. S. R. Costa, A.F. Jozala, L.O. Nascimento, P.G. Mazzola, M.V. Chaud, A.A. Vicente, A.M. Lopes, Curcumin encapsulation in nanostructures for cancer therapy: a 10-year overview, *International Journal of Pharmaceutics* (2021), doi: https://doi.org/10.1016/j.ijpharm.2021.120534

This is a PDF file of an article that has undergone enhancements after acceptance, such as the addition of a cover page and metadata, and formatting for readability, but it is not yet the definitive version of record. This version will undergo additional copyediting, typesetting and review before it is published in its final form, but we are providing this version to give early visibility of the article. Please note that, during the production process, errors may be discovered which could affect the content, and all legal disclaimers that apply to the journal pertain.

Curcumin encapsulation in nanostructures for cancer therapy:
a 10-year overview

Natália A. D'Angelo[1]; Mariana A. Noronha[1]; Isabelle S. Kurnik[2];

Mayra C. C. Câmara[1]; Jorge Vieira[3]; Luís Abrunhosa[3]; Joana T. Martins[3];

Thais F. R. Alves[4,5,6]; Louise L. Tundisi[1]; Janaina A. Ataide[1]; Juliana S. R. Costa[1];

Angela F. Jozala[7]; Laura O. Nascimento[1]; Priscila G. Mazzola[1]; Marco V. Chaud[4,5,6];

António A. Vicente[3]; Andre M. Lopes[1*]

[1]Faculty of Pharmaceutical Sciences, State University of Campinas (UNICAMP), Campinas, Brazil.

[2]School of Pharmaceutical Sciences, São Paulo State University (UNESP), Araraquara, Brazil.

[3]Centre of Biological Engineering (CEB), University of Minho, Braga, Portugal.

[4]Laboratory of Biomaterials and Nanotechnology (LaBNUS), University of Sorocaba, Sorocaba, Brazil.

[5]College of Engineering of Bioprocess and Biotechnology, University of Sorocaba, Sorocaba, Brazil.

[6]Sorocaba Development and Innovation Agency (INOVA Sorocaba), Sorocaba Technology Park, Sorocaba, Brazil.

[7]Laboratory of Industrial Microbiology and Fermentation Process (LAMINFE), University of Sorocaba, Sorocaba, Brazil.

*Corresponding author:

Dr. André M. Lopes

amlopes@unicamp.br

Faculty of Pharmaceutical Sciences,

State University of Campinas (UNICAMP)

Abstract

Curcumin (CUR) is a phenolic compound present in some herbs, including *Curcuma longa* Linn. (turmeric rhizome), with a high bioactive capacity and characteristic yellow color. It is mainly used as a spice, although it has been found that CUR has interesting pharmaceutical properties, acting as a natural antioxidant, anti-inflammatory, antimicrobial, and antitumoral agent. Nonetheless, CUR is a hydrophobic compound with low water solubility, poor chemical stability, and fast metabolism, limiting its use as a pharmacological compound. Smart drug delivery systems (DDS) have been used to overcome its low bioavailability and improve its stability. The current work overviews the literature from the past 10 years on the encapsulation of CUR in nanostructured systems, such as micelles, liposomes, niosomes, nanoemulsions, hydrogels, and nanocomplexes, emphasizing its use and ability in cancer therapy. The studies highlighted in this review have shown that these nanoformulations achieved higher solubility, improved tumor cytotoxicity, prolonged CUR release, and reduced side effects, among other interesting advantages.

Keywords: curcumin (CUR); drug delivery systems (DDS); bioactive encapsulation; nanotechnology; cancer therapy; nanostructures.

Graphical abstract

These figures are not on the same scale.
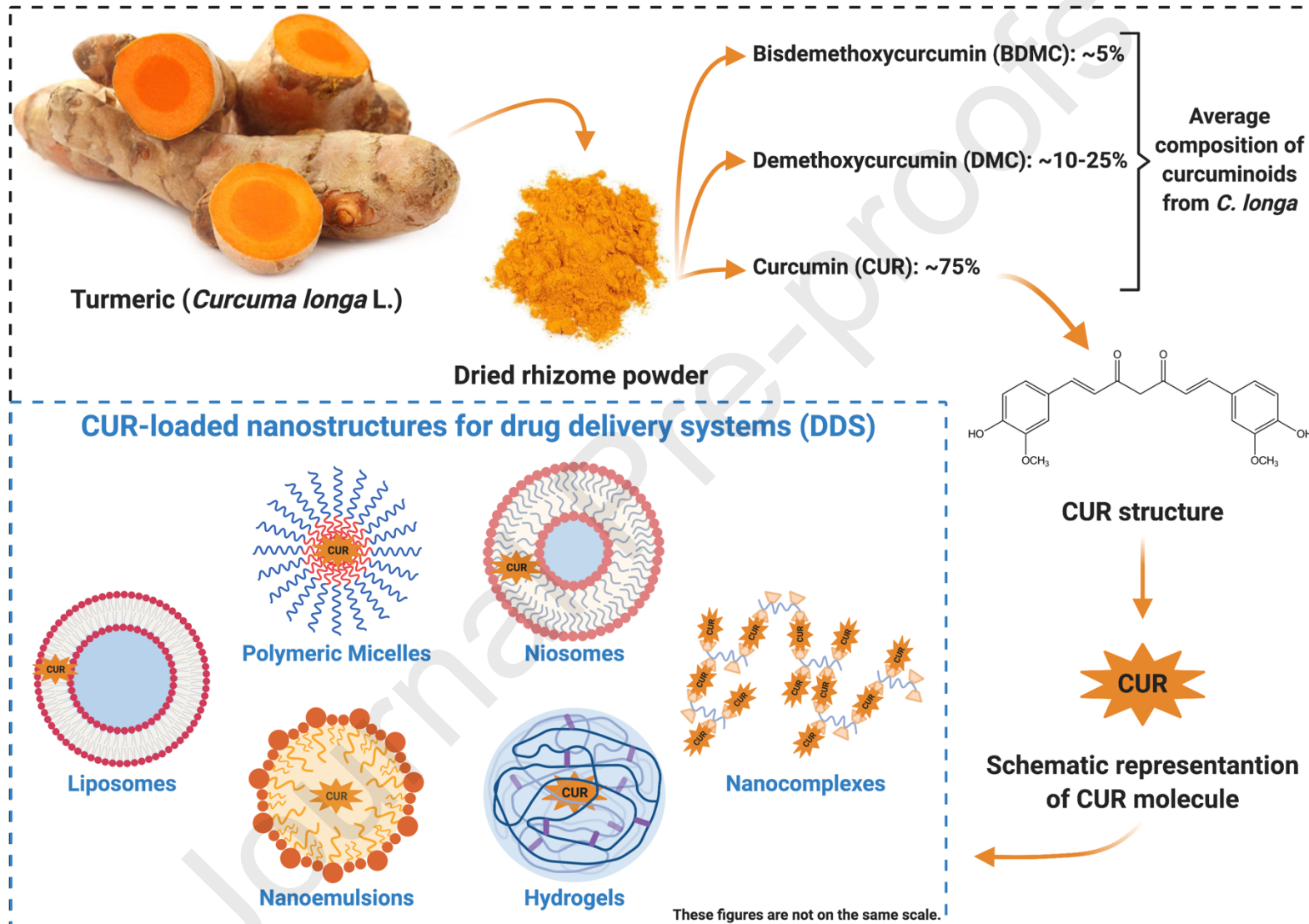
1. Introduction

Curcumin (CUR) is a bioactive compound and the main fraction derived from curcuminoids extracted from turmeric (*Curcuma longa* L.) rhizomes, a ginger family member (Zingiberaceae). This molecule is also known as Diferuloylmethane. The curcuminoids from *C. longa* have been extensively studied because of their anti-inflammatory and antioxidant properties, and their potential activity as antitumoral, antibacterial, antioxidant, anti-inflammatory, antiviral, and antifungal agents (Abdel-Wahhab et al., 2016; Alavi et al., 2018; Pushpalatha et al., 2019; Zielińska et al., 2020a). However, the dietary and pharmacological application of native CUR is hindered due to poor water solubility and chemical instability, resulting in low bioavailability, fast metabolism, and predisposition to photochemical degradation (Alves et al., 2019; Altunbas et al., 2011; Olotu et al., 2020; Yallapu et al., 2012; Wang et al., 2016). One way to overcome these drawbacks can be the encapsulation of CUR to improve its water-solubility, stability, and consequently, the bioavailability of this phenolic compound.

One of the first studies related to CUR encapsulation in nanostructures (Ns) was published by Kuttan et al. (1985). These authors studied the encapsulation of CUR in liposomes (composed of phosphatidylcholine and cholesterol) and showed that after administering 1 mg of the nanoformulation (*i.e.*, 50 mg/kg) per mouse, all animals survived up to 30 days, and only two of them developed tumors and died before 60 days. It was also observed that encapsulated CUR showed significantly higher capacity as an anticancer agent against Dalton's lymphoma cells than free CUR. After that, the scientific research involving the encapsulation of CUR to improve its pharmacokinetics and systemic bioavailability has grown considerably in the last years. However, most published works focus mainly on CUR therapeutic effects.

Comparative studies that address the stability of nanoencapsulated CUR and studies that effectively address the production engineering of Ns loaded with CUR are scarce or incomplete. Such studies are necessary to maximize Ns performance and enable their scale-up production.

Many (bio)materials such as polymers, amphiphilic copolymers, surfactants, lipids, and proteins have been evaluated as encapsulation matrices due to their biocompatibility, biomimesis, and biodegradability, with non-toxic metabolites upon physiological degradation (Naksuriya et al. 2014; Rafiee et al., 2018; Zielińska et al., 2020b). In addition, the encapsulation of hydrophobic bioactive compounds such as CUR in Ns can render these compounds more hydrosoluble than their free counterparts, opening possibilities for more administration routes, including intravenous. Thus, nanobiotechnology provides a flexible method to overcome the limitations mentioned above, *e.g.*, the poor water solubility of lipophilic bioactive compounds.

In this context, our focus in this work is to review the main aspects of CUR as a potential bioactive in nano-based drug delivery systems (DDS), including the characteristics, properties, and mechanism of action of this molecule, with a particular emphasis on its antitumor properties, as well as the latest developments regarding the Ns most employed for its encapsulation, focusing on works published during the last 10 years. In the following sections, we also review therapeutic and pharmacological data of CUR loaded DDS, with a special emphasis on therapy against cancer.

2. Characteristics, properties, and mechanism of action of curcumin

Indian spice turmeric (*C. longa*) contains a mixture of curcuminoids, turmerin, and some essential oils (*e.g.*, zingiberene, turmerones, and atlantones). Curcuminoids

represent only a fraction of approximately 2-9% of the total extract. These curcuminoids belong to the diferuloylmethane group of phenolic compounds and consist of CUR, demethoxycurcumin (DMC), and bisdemethoxycurcumin (BDMC), with respective fractions of about 75, 10-20, and 5% (Patil et al., 2019; Ukrainczyk et al., 2016). These three major curcuminoids have similar chemical structures, distinguished only by the presence or absence of a methoxy functional group attached to each of the aromatic rings (Heffernan et al., 2017), as can be seen in Figure 1.
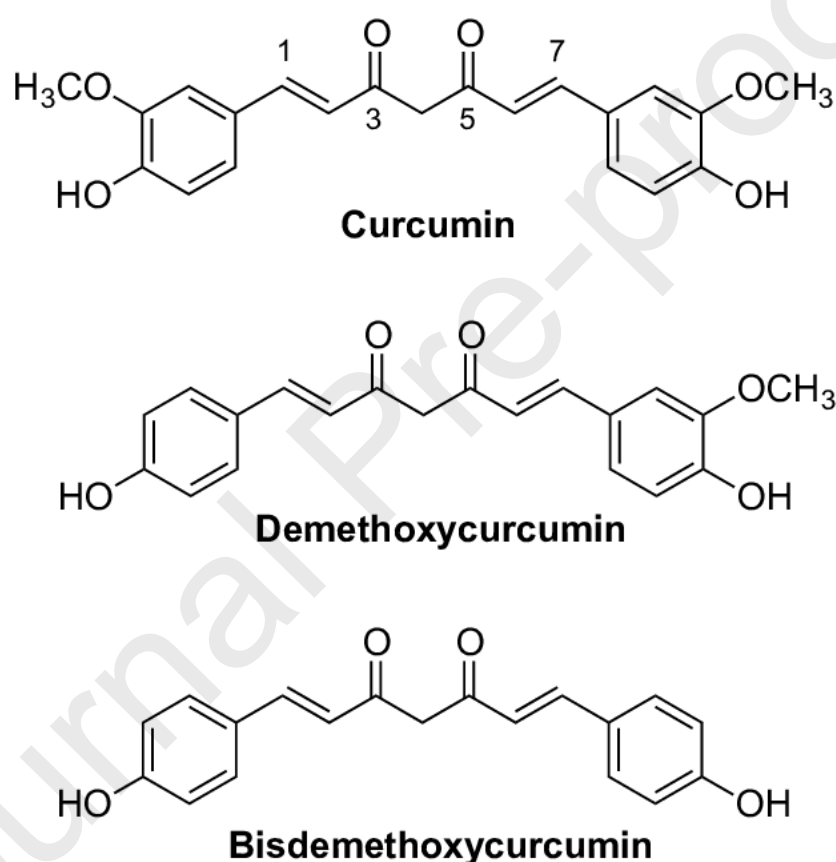

Figure 1. Chemical structures of curcumin (**a**), demethoxycurcumin (**b**), and bisdemethoxycurcumin (**c**) displaying the differences in the R_1 and R_2 groups between the three curcuminoids. Based on Heffernan et al. (2017).

CUR, in its pure form, is a solid crystalline compound with a golden-yellow color. Its IUPAC name is 1,7-bis(4-hydroxy-3-methoxyphenyl)1,6-heptadiene-3,5-dione, its chemical formula is $C_{21}H_{20}O_6$ and show an average molecular mass of 0.36838 kDa.

CUR physicochemical characteristics include melting point at ~183°C, predicted log P of 3.2 (XLogP3-AA method), UV spectral peak (maximum in ethanol) at 426 nm, and two isomers. Other properties can be found in details in the following works or platforms: ChemSpider; DrugBank; Kotha and Luthria (2019); Kurnik et al. (2020; 2021); Moghadamtousi et al. (2014); Patel et al. (2020); Prasad and Aggarwal (2011); PubChem; and Salem et al. (2014).

CUR can interfere with diverse biochemical pathways involved in the proliferation and survival of cancer cells by directly and indirectly binding to different targets. As highlighted by Salem et al. (2014), cancer has several molecular markers involved in its onset and progression. This molecule has been shown to interact with various targets, including transcription factors, growth factors, DNA, RNA, and several proteins involved in cell signal transduction pathways (Gupta et al., 2013; Shehzad et al., 2013a). CUR's mechanism of action can occur both intrinsically (mitochondrial) and extrinsically (mediated via cell surface transmembrane death receptors) (Shehzad et al., 2013b). The suggested pathways by which CUR shows anticancer properties have been described in detail in several interesting reviews (Epstein et al., 2010; Gupta et al., 2011; 2013; Patel et al., 2020; Salem et al., 2014; Shehzad et al., 2013a).

In particular, the antitumoral effect of CUR is highly related to its anti-inflammatory effect. As highlighted by Alves et al. (2019) and Edwards et al. (2017), this effect is associated with the influence that this bioactive compound has on molecules involved in the cellular inflammation process, such as pro-inflammatory molecules, proteolytic enzymes, and cytokines. CCM can inhibit the production of interleukin 1 (IL-1), IL-6, IL-8, and IL-12, as well as tumor necrosis factor α. The effects of CCM on pro-inflammatory molecules may be associated with inhibition of the formation of arachidonic acid, an important eicosanoid substrate. CCM may also

7

inhibit the activity of enzymes such as cyclooxygenases and lipoxygenase, and the production of inflammatory mediators (prostaglandins). Based on in this anti-inflammatory effect, as well as antioxidant and antitumoral properties, different CUR formulations have been developed and commercialized in the last years, such as: Meriva®, Cavacurmin®, Cureit®; Acumin®, Gelucire®, and BioCurc®. For more examples, we recommend the following works (Belcaro et al. 2014; Stohs et al., 2020).

Throughout the years, CUR effect on tumor cells has attracted significant attention and workload. In this context, we prepared a list of the most significant works related to different types of cancer treatments using CUR (Table 1).

Table 1. Summary of curcumin approach to cancer therapy in different types of tumor cells (according to cell line), as reported in the literature in the last 10 years.

Type of cancer and cell lines tested	References
Breast cancer (HCC-38, UACC-3199, and T47D) cells	Al-Yousef et al. (2020)
Leukemia (K562) cell	Lestari et al. (2019)
Bladder cancer (T24 and UMUC2) cells	Tian et al. (2017)
Colon adenocarcinoma (COLO 320DM) cell	Dasiram et al. (2017)
Skin cancer (melanoma)	Lelli et al. (2017)
Prostate cancer (DU145, PC3, and RPWE-1) cells	Cao et al. (2017)
Lung cancer (A549) cell	Liu et al. (2017)
Lung cancer (A549 and H1299) cells	Zhu et al. (2017)
Leukemia (SHI-1) cell	Zhu et al. (2016)
Breast cancer (MCF-7) cell	Wang et al. (2016)
Lung cancer (A549 and PC-9) cells	Jiao et al. (2016)
Skin squamous carcinoma (A431) cells	Wu et al. (2015)
Skin cancer [BK5.IGF-1 transgenic mice that overexpress insulin-like growth factor-1 (IGF-1) in the skin epidermis]	Kim et al. (2014)
Human glioblastoma multiforme [A172, KNS60, U251MG(KO)] cells and medulloblastoma (ONS76) cell	Khaw et al. (2013)
Papillary thyroid cancer (K1) cell	Zhang et al. (2013)
Cervical cancer (HeLa, SiHa, CaSki, and C33A) cells	Singh and Singh (2011)

In this section, our objective was to show general characteristics, properties, as well as CUR mechanisms of action and not to make an in-depth discussion about each

specific topic. For more details by the interested reader in other therapeutic effects, we recommend the excellent following works: for antibacterial effect (Olszewska et al., 2020; Prasad and Aggarwal, 2011; Tyagi et al., 2015; Winter et al., 2013); for antifungal effect (Garcia-Gomes et al., 2012; Lee and Lee, 2014; Neelofar et al., 2011; Sharma et al., 2010); and for antiviral effect (Dai et al., 2018; Mathew and Hsu, 2018; Moghadamtousi et al., 2014; Mounce et al. 2017).

3. Limitations of curcumin administration

Oral administration for systemic effects presupposes minimum water solubility, chemical stability under acidic (stomach) or around neutral pH (terminal jejunum and ileum), and mucosal absorption. CUR is practically water-insoluble (approximately 1.34 mg/L) (Carvalho et al., 2015), unstable in neutral and mildly alkaline pH conditions (*e.g.*, ~25% degradation after 10 h in pH 8.0 at 25°C) and presents debatable stability under acidic pH (Kurnik et al., 2020; Martínez-Guerra et al., 2019; Schneider et al., 2015). For more details about its instability and degradation aspects, we recommend the interesting works of Alves et al. (2019) and Salem et al. (2014). As expected from its physicochemical profile, CUR demonstrates low bioavailability after oral ingestion, and is mostly found in feces. Clinical trials that evaluated CUR oral intake (0.5 to 12 g/day), found CUR in the plasma with peak levels between 1-2 h, and traces or undetectable CUR up to 2 g/day. Studies vary on their dosage forms (tablets/capsules and food), different food intake regimes (empty stomach, with fat-rich meals, etc.), and CUR source (chemically synthesized, standardized extracts with other curcuminoids). Therefore, comparisons of peak levels between them should be cautious. Low plasma levels also derive from an extensive CUR metabolism mainly in the liver, followed by intestine and gut microbiota. However, several metabolic products also have

pharmacological properties, so metabolism itself may not impair treatment efficacy (Dei Cas and Ghidoni, 2019).

CUR low percutaneous permeation does not favor skin as an alternative route for its administration. However, an *in vitro* study with rat skin showed that CUR microemulsion substantially increased its permeation while emulsions had little effect, and demonstrated that transdermal application was possible by decreasing droplets' average size (Sintov, 2015). In blood, CUR seems to be highly stable by binding to human serum albumin and fibrinogen because it precludes its degradation through hydrolysis (Leung and Kee, 2009). Also, CUR binding to bovine serum albumin (BSA) did not hamper *in vitro* CUR antioxidant and antiproliferative activities on cancer cells (Mirzaee et al., 2019). Therefore, CUR parenteral administration would pose solubility drawbacks. Despite this, toxicity studies in clinical trials find no limitations to CUR oral administration in humans so far, having been classified as Generally Recognized as Safe (GRAS). Noteworthy, an *in vitro* study using high CUR concentrations (10 to 40 µg/mL) induced mitochondrial and nuclear DNA damage in human hepatoma G2 cells, but the phenomenon was not observed *in vivo* (Damarla et al., 2018).

In this context, in order to enhance CUR potential as a therapeutic agent in face of the above considerations, CUR encapsulation in Ns is an excellent alternative, not only to facilitate its absorption by the organism but also to protect it from degrading agents. Moreover, other characteristics such as the bioavailability and/or modified release can be improved by the use of Ns, and even properties such as the stability of CCM exposed to light can also be increased with nanoformulations. The surface of Ns allows different molecules to be attached to its structure [*i.e.*, PEGylation, affinity ligands (*e.g.*, transferrin and folate), imaging agents, among others], resulting in better targetability to the target site (*e.g.*, cancer cells). In fact, the interesting stabilization

that nanoformulations offer for this molecule seems to be related to the hydrophobic interactions between CUR and the hydrophobic branches of the material/biomaterial which constitute the different Ns. This effect eliminates or considerably reduces interactions with water molecules in the medium, reducing or inhibiting the degradation of CUR by hydrolysis. As result, nanoformulations approach can allow the administration of CUR through different routes, such as mucosal, intravenous, oral, and topical. In addition, high plasma concentrations can be achieved with lower dosages, reducing side effects and maintaining therapeutic efficacy (Alves et al., 2019; Li et al., 2014; Salem et al. 2014; Zielińska et al., 2020a).

4. Main nanostructures for curcumin encapsulation

The Ns referred in this section increase CUR solubility and, at the same time, protected CUR against hydrolysis, enzymatic reduction, and conjugation inactivation, amongst others. Some nanoformulations aim prolonged CUR release, while others focus on targeting, using additional cellular delivery mechanisms or intracellular release. A formulation efficiently prepared and loaded should be capable to retain CUR for the required period.

The Ns selected by our research group to be discussed here are organic Ns, such as micelles, liposomes, niosomes, nanoemulsions, hydrogels, and nanocomplexes. This choice is based on the main discoveries using these Ns, as well as in our interest in these nanocarriers. Although an excellent work published by Naksuriya et al. (2014) emphasized the pharmaceutical properties, preclinical studies, and clinical data related to cancer treatment with CUR nanoformulations, a considerable amount of works were published the last 6 years that enlighten mechanism, structures or bring innovative solutions to this subject. Our focus here

was not to show the processes and techniques employed in obtaining Ns, but to show and compare the main results of CUR encapsulation in Ns, such as: size (nm); polydispersity index (PDI); zeta (ζ) potential; drug loading (%*DL*); efficiency of encapsulation (%*EE*); CUR release profile; and *in vitro*/*in vivo* cytotoxicity studies against tumor cells.

4.1. Micelles

Polymeric micelles (PMs) have gathered significant interest as DDS because of their low toxicity, good biocompatibility, modified release pattern, increased blood circulation time, and ability to solubilize hydrophobic drugs such as CUR in the micelles' core (Akbar et al., 2018). The hydrophobic segments in the polymers/copolymers form the micelle core that acts as a reservoir for hydrophobic drugs, while the hydrophilic headgroups form the micellar shell that can improve the colloidal stability and prevent protein adsorption, thus prolonging the circulation time (Gou et al., 2011; Zhao et al., 2020). In particular, one type of material that is used as a biocompatible complexing agent to improve the water solubility, stability, and bioavailability of poor aqueous soluble drugs is Pluronic® copolymers, which contain hydrophobic poly(propylene oxide) (PPO) blocks and hydrophilic poly(ethylene oxide) (PEO) blocks arranged in a triblock structure, PEO-PPO-PEO. These attractive mixed PMs may be used as pharmaceutical carrier for CUR and other hydrophobic drugs (Akbar et al., 2018). Figure 2 shows the PMs structure with CUR encapsulated in its hydrophobic core.
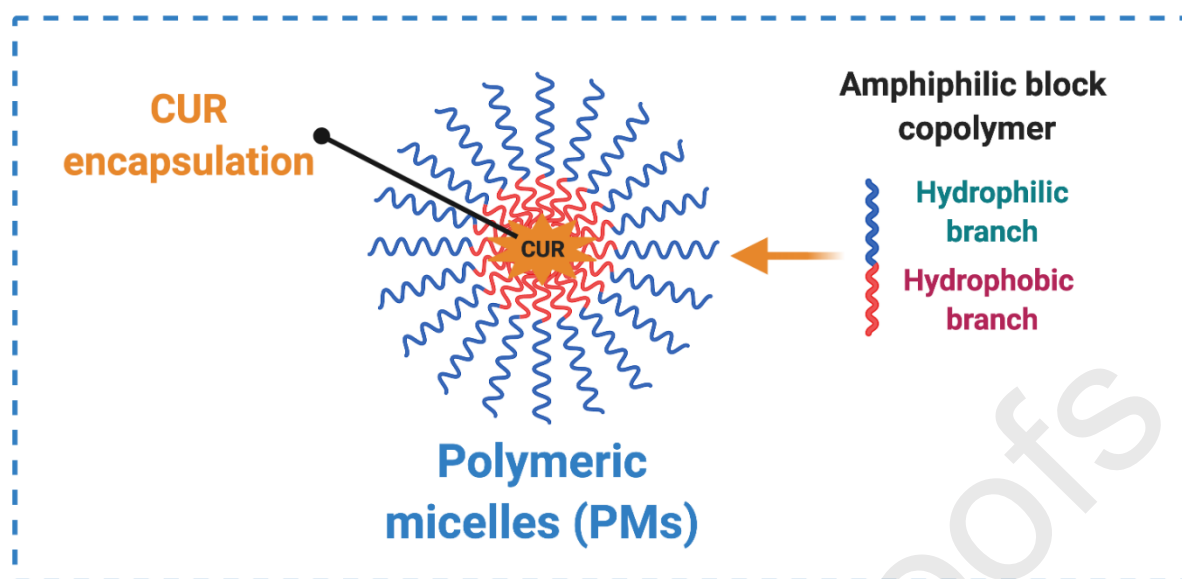
Figure 2. Schematic representation of polymeric micelles (PMs) obtained by amphiphilic copolymers. PMs can be spherical or cylindrical, with a hydrophobic core and hydrophilic surface and significantly more stable than surfactant-based micelles, based on Pachioni-Vasconcelos et al. (2015).

PMs are the Ns most used for encapsulating CUR as DDS for cancer therapy. In this section, we briefly present some research works employing CUR in PMs against tumor cells. Zhao et al. (2020) presented a redox-sensitive micellar system to overcome the multidrug resistance in cancer cells. Doxorubicin (DOX) and CUR were co-conjugated onto a zwitterionic polymer, poly(carboxybetaine) (pCB), to form CUR-pCB-DOX that self-assembled into stable micelles. Those micelles presented a mean particle size of 164.2 nm, ζ potential of +32.1 mV, and PDI of 0.436, showed high colloidal stability in 10% fetal bovine serum solution at 37°C, and exerted significantly stronger antitumor activity against human mammary adenocarcinoma MCF-7 and MCF-7/Adr *in vitro* than individual delivery formulation (*i.e.*, pCB-DOX + pCB-CUR) at the same concentrations of both drugs. Moreover, there was a significant reduction in the half-maximal inhibitory concentration (*IC*$_{50}$) value of pCB-DOX (14.1 µg/mL) compared to the free DOX value (437.2 µg/mL), and co-delivery of pCB-DOX with

pCB-CUR further reduced the IC_{50} value to 8.9 µg/mL. Also, CUR-pCB-DOX exhibited the strongest cytotoxicity effect against MCF-7/Adr cells (5.87 µg/mL). The conjugate cellular uptake was enhanced due to the increased permeability and retention effect of tumor cells on the micellar conjugate.

Lachowicz et al. (2019) synthesized, in a simple one-step process *via* Steglich esterification, a bioconjugate of sodium alginate and CUR (AA-CUR), and used this to prepare stable calcium cross-linked spherical micelles serving as a delivery vehicle for CUR. The AA-CUR PMs showed a particle size of 200 nm, with high colloidal stability (ζ = -53.0 mV) and PDI of 0.200. Prolonged release of CUR was achieved for PMs during 5 h under physiological conditions (pH 7.4, at 37°C), with ~62 and 95% of CUR being released after 1 and ~4 h, respectively. To assess AA-CUR PMs cytotoxicity, mouse cancer cell lines from mammary carcinoma 4T1, melanoma B16F10, and colon carcinoma CT26-CEA and MC38-CEA were used. A dose-dependent sensitivity of all tested cancer cells to AA-CUR was observed. The IC_{50} values were 0.35, 0.175, 0.175, and 0.35 mg/mL for 4T1, B16F10, CT26-CEA, and MC38-CEA cell lines, respectively.

In another work, a dually loaded complex PM system was developed for co-delivering DOX with CUR using a classic thin-film hydration method (Zhang et al., 2018a). The *in vitro* safety and antitumor efficacy were evaluated on H9C2 cells by measuring viability and tumor growth inhibition in tumor-bearing mice, respectively. The results showed a %*DL* of 8.1% for CUR and 2.6% for DOX, and 98% of %*EE* for both CUR and DOX. The averaged particle size of freshly prepared nanoformulation was 35.7 nm with a mean PDI of 0.09, and ζ potential of -2.28 mV. The release profile was investigated for both drugs using PBS containing 0.5% Tween 80 at pH 3.5 as the medium to maintain the chemical stability during quantification. DOX showed a higher cumulative release rate (75%) than CUR (40%) within 72 h.

Luong et al. (2017) developed nanomicelles composed of folic acid, styrene-maleic acid, and curcumin–difluorinated (FA-SMA-CDF). In the active targeting approach, nanomicelles are typically conjugated/decorated with a targeting moiety, thereby facilitating the preferential accumulation of the drug in selected tissues, individual cancer cells, or intracellular organelles associated with specific recognition molecules in cancer cells. The FA-SMA-CDF nanomicelles' size and PDI values were 191.3 nm and 0.176, respectively. Non-targeted (SMA-CDF) and targeted (FA-SMA-CDF) nanoformulations had negative ζ potential values of -50.79 and -7.86 mV, respectively. The CDF loading in SMA-CDF and FA-SMA-CDF was 18.48 and 10.44%, respectively. The IC_{50} values of CDF, SMA-CDF, and FA-SMA-CDF on SKOV 3 cells after 72 h were 0.65, 1.20, and 0.40 µM, respectively. FA-SMA-CDF micelles reduced the IC_{50} value of SMA-CDF by approximately 3-folds. A similar pattern of cell viability was observed in the case of HeLa cells, where IC_{50} values of CDF, SMA-CDF, and FA-SMA-CDF were found to be 0.70, 1.28, and 0.47 µM, respectively. Regarding A549 cells, the IC_{50} values of CDF, SMA-CDF, and FA-SMA-CDF after 72 h were 1.65, 1.85, and 1.55 µM, respectively. In this sense, the results suggested the promising potential of FA-SMA-CDF for targeted anticancer therapy.

Zheng et al. (2016) developed CUR-loaded micelles using the copolymer monomethoxy poly(ethylene glycol)-poly(lactide) (MPEG-PLA). This work aimed to explore CUR-MPEG-PLA micelles' efficiency at a cellular level by investigating the drug uptake, apoptosis, and cytotoxicity to tumor cells *in vitro*. Biodegradable CUR-MPEG-PLA micelles were applied against C6 and U251 glioma cells *in vitro* and *in vivo* to treat glioma cancer. Compared with free CUR, the cellular uptake and cytotoxicity were increased *in vitro* after CUR was encapsulated into PMs. The CUR-MPEG-PLA micelles were characterized concerning average diameter (~33 nm), PDI

(0.120), %*DL* (9.85%), %*EE* (98.5%), and ζ potential (-3.3 mV). The IC_{50} values of the nanoformulation on U251 cells were 29.02 and 6.82 µg/mL after 24 h and 48 h, respectively, while against C6 cells were 4.38 and 1.57 µg/mL after 24 h and 48 h, respectively. There was an increase of 40% in the amount of CUR released from the nanoformulation after 120 h, while the free CUR exhibited a high release level (40%) at 2 h. Furthermore, CUR-MPEG-PLA micelles showed significant effectiveness in suppressing glioma growth by inducing more cell apoptosis and inhibiting more cell proliferation and angiogenesis compared to free CUR. The authors considered that these formulations had the potential for clinical applications in glioma therapy.

The most significant results found in the literature on CUR-PMs for DDS approaches applied to cancer therapies are summarized in Table 2. The CUR-PMs nanoformulations size showed values from ~16.4 to 200 nm; the PMs with small size can sometimes exhibit long circulation times *in vivo*, which is a significant advantage for cancer therapy. In addition, the formulations were relatively monodisperse and stable, with interesting %*DL* (~3 to 16%) and %*EE* (88 to 99%) values, as can be seen in Table 2. Overall, the newly developed PMs encapsulated and delivered CUR efficiently in various cancer cell lines *in vitro* and into *in vivo* tumors, resulting in improved therapeutic efficacy of encapsulated CUR compared to treatments with free CUR. In addition to CUR, PMs could potentially be utilized to deliver any hydrophobic chemotherapeutic agents into tumors. These studies provide a strong rationale for the potential utilization of PMs as a promising anticancer therapy.

16

Table 2. Summary of curcumin-loaded polymeric micelles (PMs) approach for cancer therapy reported in the literature over the past 10 years. PDI, %*DL*, %*EE*, and *IC*$_{50}$ correspond to polydispersity index, drug loading, efficiency of encapsulation, and half-maximal inhibitory concentration, respectively.

Type of polymeric micelles systems/Composition	Size (nm)	PDI	ζ potential (mV)	%*DL*	%*EE*	*IC*$_{50}$	Release results	Cell lines evaluated	References
PMs composed by Pluronic L35 and ionic liquids	42.5 – 45.6	0.110 – 0.150	-18.4 – -14.6	14.8 –16.2	94.1 – 96.0	0.035 µM (PMs/[Ch][Hex]) 0.065 µM (PMs/[Ch]Cl)	18% (PMs/[Ch]Cl) 2% (PMs/[Ch][Hex]) Both after 2.5 h	Human prostatic carcinoma (PC3) cell line	Kurnik et al. (2021)
Redox-sensitive micelle/Doxorubicin (DOX) and CUR co-conjugated onto a poly(carboxybetaine) (pCB) **Abbr.: CUR-pCB-DOX**	164.2	0.436	+32.1	11.7 µg/mL (CUR) 64.2 µg/mL (DOX)	-	5.87 µg/mL (CUR-pCB-DOX) 8.9 µg/mL (pCB-CUR) 14.1 µg/mL (pCB-DOX) 437.2 µg/mL (free DOX)	89.7% of CUR after 30 h with 10 mM GSH 92.4% of DOX after 30 h with 10 mM GSH (both from CUR-pCB-DOX)	Human mammary adenocarcinoma (MCF-7 and MCF-7/Adr) cells	Zhao et al. (2020)
Bioconjugate of sodium alginate – CUR cross-linked with calcium	178 – 200	0.200 – 0.290	-53.0 – -25.9	-	-	0.35 mg/mL (4T1) 0.175 mg/mL (B16F10) 0.175 mg/mL (CT26-CEA) 0.35 mg/mL (MC38-CEA)	~62% after 1 h 95% after ~4 h	Mammary carcinoma (4T1), melanoma (B16F10), and colon carcinoma (CT26-CEA and MC38-CEA) cells	Lachowicz et al. (2019)
Hydrophilic hyaluronic acid-SS-CUR functionalized with Tween-80 **Abbr.: CUR-THSC**	74.2	0.160	-30.2	8.9	94.1	5.98 µg/mL (CUR-THSC) 23.84 µg/mL (free CUR) 13.76 µg/mL (CUR-THC, formulation without SS bonds)	43.2% after 24 h in GSH (pH 7.4) 22.7% after 24 h without GSH (pH 5.0) 43.2% after 24 h in GSH (pH 5.0)	Glioblastoma (G422) cells	Tian et al. (2018)

Formulation	Size (nm)	PDI	Zeta			IC50	Release	Cell line	Reference
PMs composed by Pluronics P123 and PF127 (best formulations: F2 and F10)	16.93 (F2) 16.39 (F10)	-	-8.51 (F2) -18.7 (F10)	~10 (F2) ~10 (F10)	~96 (F2) ~99 (F10)		-	Human cervical cancer (HeLa) cells	Akbar et al. (2018)
Complex PMs co-encapsulating DOX and CUR	35.7	0.090	-2.28	8.1 (CUR) 2.6 (DOX)	98 (both)	-	40% after 72 h (CUR) 75% after 72 h (DOX)	*In vitro* viability of H9C2 cells, and tumor growth inhibition in tumor-bearing mice	Zhang et al. (2018a)
PMs/composed by Poloxamers (P188 and P407) **Abbr.: CUR-P188 and CUR-P407**	30.3 (CUR-P4–7 - the best formulation obtained) 139 (CUR-P188)	~0.324	-	2.94	88.4	5.7 µg/mL (CUR-P407) 9.7 µg/mL (CUR-DMSO)	7% after 24 h 45% after 72 h (CUR-P407) 76% after 24 h 87% after 72 h (CUR-DMSO)	Human eosinophilic leukemia (EoL-1) cells	Tima et al. (2017)
Folic acid – styrene-maleic acid – curcumin – difluorinated	191.3	0.176	-7.86	10.44	-	0.40 µM (SKOV) 0.47 µM (HeLa) 1.55 µM (A549)	-	Human ovarian carcinoma (SKOV3), human cervical cancer (HeLa), and human lung cancer (A549) cells	Luong et al. (2017)
Cholesterol (Ch)-modified methoxy-polyethylene glycol-poly(lactic acid) (mPEG-PLA) polymer	104.6 (mPEG-PLA) 169.3 (mPEG-PLA-Ch)	0.300 – 0.488	-18.2	11.86	93.74	-	69.83% after 24 h	Murine melanoma (B16F10) and human breast cancer (MDA-MB-231) cells	Kumari et al. (2017)
PMs composed by biodegradable monomethoxy poly(ethylene glycol)-poly(lactide) copolymers **Abbr.: CUR-MPEG-PLA**	~33	0.120	-3.3	9.85	98.5	29.02 µg/mL after 24 h 6.82 µg/mL after 48 h (with CUR-MPEG-PLA both to U251) 43.37 µg/mL after 24 h 10.38 µg/mL after 48 h (with free CUR both to U251)	25% after 24 h >40% after 120 h	Glioma (C6 and U251) cells	Zheng et al. (2016)

					4.38 µg/mL after 24 h 1.57 µg/mL after 48 h (with CUR-MPEG-PLA both to C6) 4.74 µg/mL after 24 h 1.97 µg/mL after 48 h (with free CUR both to C6)			
PMs composed by monomethoxy poly(ethylene glycol)-poly(ε-caprolactone) diblock copolymer **Abbr.: CUR-MPEG-PCL**	27.3	0.097	-	~13	99.1	5.78 µg/mL (CUR-MPEG-PCL) 3.95 µg/mL (free CUR)	54.6% after 9 days	Colon carcinoma (C-26) cell	Gou et al. (2011)

"-" this parameter was not reported by the authors;

[Ch][Hex]: cholinium hexanoate, and [Ch]Cl: cholinium chloride;

Abbr.: Abbreviation of the formulation used by the authors;

GSH: overexpressed glutathione; DMSO: dimethyl sulfoxide; and DTT: dithiothreitol.

4.2 Liposomes

Liposomes (LSs) are self-assembled systems. They are colloidal nano- to micro-sized vesicles, having at least a lipid bilayer that encloses an aqueous core. The wall of LSs is made of phospholipids purified from natural or synthetic sources, and it can incorporate hydrophilic, hydrophobic, and photo-instable drugs as illustrated in Figure 3a (Momoh and Esimone, 2012; Riaz et al., 2018; Sercombe et al., 2015). The natural phospholipid sources are phosphatidylserine and phosphatidylcholine, which can be obtained from soy and egg yolk, respectively. The synthetic phospholipids are synthesized from glycerol-phosphocholine and maintain the stereochemical configuration of its molecule-pair from the natural source (van Hoogevest, 2017). Some of them can be previously designed for a specific function from PEG-lipid conjugates incorporating functionalized PEG termini, like amine, carboxylic acid, azide, aldehyde, thiol, and hydroxy (Figure 3b). The PEGylated systems are a valuable strategy for creating a steric stabilization effect at the surface of LSs, increasing repulsive forces between LSs and serum-components (Dhule et al., 2012). Moreover, modified LSs have also been highlighted as a multifunctional theragnostic agent for multimodal imaging, induced photodynamic therapy (PDT) (Figure 3c), hypoxia-activated cancer therapy, and trigger chemotherapy, resulting in a significantly improved efficacy compared to conventional cancer PDT (Feng et al., 2017).
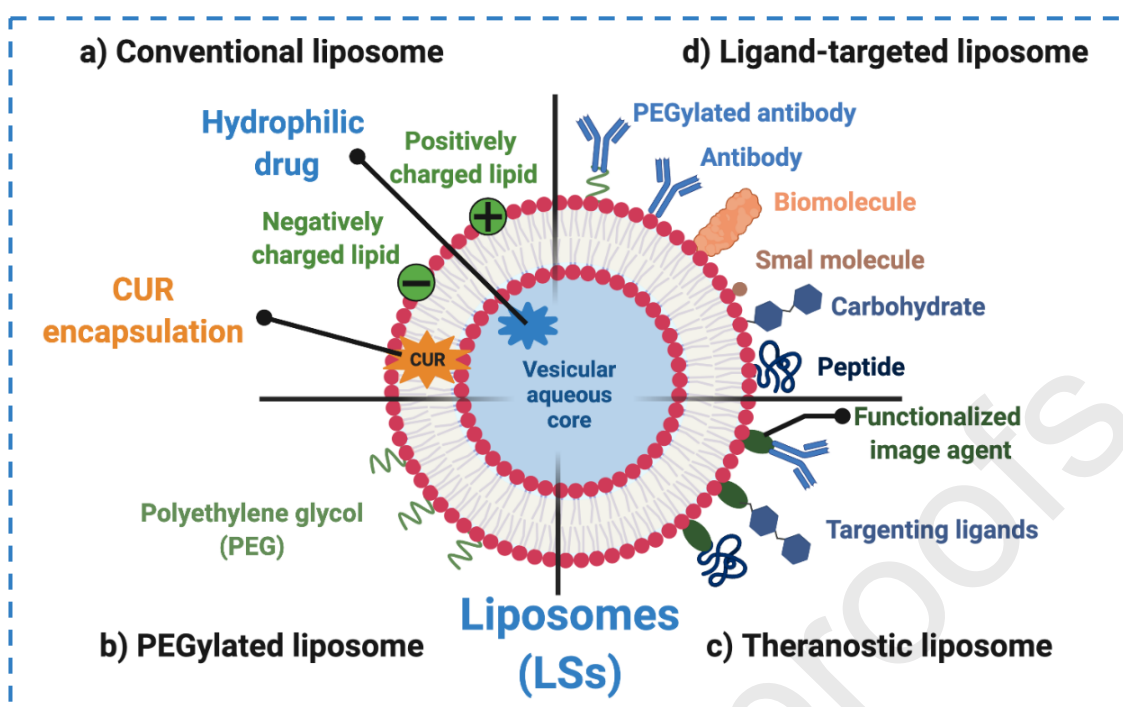
Figure 3. Schematic diagram of liposomes (LSs): (**a**) conventional LSs are made of phospholipids; (**b**) PEGylated/stealth LSs contain a layer of polyethylene glycol (PEG) at the surface of LSs; (**c**) theranostic LSs contain image agents with multifunctional characteristics; (**d**) targeted LSs contain a specific targeting ligand to target a specific site. Based on Sercombe et al. (2015).

As shown in Figure 3d, to achieve LSs manifold functionalization, a suitable ligand, peptide, antibody or their fragments, aptamer, small molecule, protein, and carbohydrate are requested for DDS (Riaz et al., 2018; Sercombe et al., 2015). The termini groups attached to the PEG-modified functional coatings improves LSs biopharmaceutical properties by increasing its circulation time, often by avoiding uptake by the reticuloendothelial system, by improving its accumulation and cellular internalization, and amplifying the therapeutic response at the surface of the tumor cells.

The LSs surface modification, as well as the size and number of bilayers as detailed in Figure 3e can be used to control LSs properties in a convenient way and get several different functions arranged simultaneously, especially to

assist drug delivery in cancer areas and overcoming CUR drawbacks in conventional pharmacotherapy, by enhancing its bioavailability, circulation time, and reducing its photo-instability.

Probably, LSs are the most used structures for CUR encapsulation, after micelles. In this context, we discussed here some works related to CUR within liposomal nanoformulation. Xu et al. (2018) developed an LS composed of soybean phosphatidylcholine, cholesterol, and CUR (CUR-LS) for endometrial carcinoma treatment. According to DLS analyses, the average particle size, PDI, and the ζ potential of the CUR-LS were 126 nm, 0.057, and -8.88 mV, respectively. The IC_{50} values of CUR-LS against human endometrial carcinoma Ishikawa and HEC-1 cell lines were 52.8 and 80.8 µM, respectively. CUR-LS treatment suppressed the activation and/or expression of nuclear factor kappa B (NF-κB), caspase-3, and matrix metalloproteinase-9.

Zhang et al. (2018b) developed a liposomal curcumin dry powder inhaler (LCDs) obtained by freeze-drying, composed of soybean lecithin and cholesterol, to treat primary lung cancer by inhalation. According to DLS analyses, the average particle size and PDI of LCDs nanoformulation were 94 nm and 0.260, respectively. This formulation had a mass mean aerodynamic diameter of 5.81 µm and a fine particle fraction of 46.7%, and was suitable for pulmonary delivery than CUR powders due to the high lung deposition of LCDs. The IC_{50} value for A549 cells was 20 µmol/L, and the low cytotoxicity on normal human bronchial BEAS-2B epithelial cells yielded a high selection index partly due to increased cell apoptosis. This formulation showed to be a promising inhalation treatment for lung cancer with high therapeutic efficiency.

CUR-LS surface modified with hyaluronic acid can target a cell-surface glycoprotein involved in cell-cell interactions (CD44) and provide effective treatment in acute myeloid leukemia by inhibiting cell growth. These modified CUR-LSs generated caspase-dependent apoptosis, inhibition of the activation of protein kinase B (Akt), and the extracellular expression of the signal-regulated kinase (ERK), also impacting the Akt/ERK signaling pathways. This strategy has been adopted by Sun et al. (2017), who developed a novel LSs system functionalized with hyaluronic acid and composed by a combination of 1,2-dimyristoly snglycero-3-phosphocholine (DMPC), 1,2-dimyristoyl-sn-glycero-3-[phospho-rac-(1-glycerol)] (DMPG), amine 1,2-distearoyl-sn-glycero-3-phosphoethanolamine-N-[amino(polyethylene glycol)-2000] (DSPE-PEG 2000), 1,2-distearoyl-sn-glycero-3-phospho-rac-glycerol (DSPE) and cholesterol, named as HA-CUR-LSs. This nanoformulation showed an average particle size, PDI, and ζ potential of 236 nm, 0.232, and -36.8 mV, respectively. Regarding CUR encapsulation, the %*DL* and %*EE* showed values of 13.2 and 66%, respectively. The CUR released *in vitro* was 60.0% and 95% after 48 and 144 h, respectively. Moreover, the *IC*$_{50}$ for acute myeloid leukemia cells was 10.9 µM, indicating that HA-CUR-LSs enhanced the antitumor potency of CUR *via* this liposome formulation with HA modification.

CUR and DOX association into LS also demonstrated antitumor efficacy against colorectal cancer (Sesarman et al., 2019). These authors developed a PEGylated CUR-LS associated with DOX, with LSs composed of dipalmitoylphosphatidylcholine (DPPC), PEG-2000-DSPE, and cholesterol. According to the results obtained, the average particle size, PDI, and ζ potential were 171 nm, 0.033, and -48.7 mV, respectively. The %*DL* and %*EE* values were

0.72 and 99.4%, respectively, and the CUR release from the LSs after 24 h was of 20%. CUR-DOX-LS showed an inhibition of the main tumor microenvironment-mediated protumour processes such as angiogenesis, inflammation, oxidative stress, invasion, and resistance to apoptosis, as well as to the alteration of T helper cells (Th1/Th2) axis in C26 colon carcinoma milieu, which favored the antineoplastic phenotype of cells.

Table 3 summarizes the most significant LS-based delivery systems of CUR developed during the last 10 years and used to treat different cancer types. LSs are versatile nanocarriers, since they enable the encapsulation of hydrophilic and hydrophobic drugs in their nanostructure, however, in general they are larger than PMs, for example. According to Table 3, the LSs size displayed values of 86 to 414 nm, many of these values being greater than 200 nm. The large size (>200 nm) can result in clearance by the reticuloendothelial system, consequently eliminating the molecule from the bloodstream (Wang et al., 2013). In summary, the liposomal nanoformulations highly enhance the effect of CUR by overcoming the water solubility limit and increasing cell endocytosis. Moreover, LSs show to be an effective carrier to enhance the stability, bioavailability, and targeting properties of CUR.

Table 3. Summary of curcumin-loaded liposomes (LSs) approach for cancer therapy reported in the literature over the past 10 years. PDI, %*DL*, %*EE*, and *IC*$_{50}$ correspond to polydispersity index, drug loading, efficiency of encapsulation, and the half-maximal inhibitory concentration, respectively.

Type of liposomes systems/Composition	Size (nm)	PDI	ζ potential (mV)	%*DL*	%*EE*	*IC*$_{50}$	Release results	Cell lines evaluated	References
Thiolated chitosan coating liposome/L-α-phosphatidylcholine, cholesterol	414	-	+37.3	3.96	88.7	-	76.6% after 12 h	Human breast cancer (MCF 7) cells	Li et al. (2020)
Aptamer A15 coating liposome/egg phosphatidylcholine, DSPE-PEG (2000), and cholesterol	86	0.210	-26.2	6.2	92.3	-	68.0% after 48 h	Human prostate cancer (DU145) cells	Ma et al. (2019)
PEGylated coating/DPPC, DSPE-mPEG-2000, and cholesterol	171	0.033	-48.7	0.72 (CUR) 0.50 (DOX)	99.4 (CUR) 44.3 (DOX)	-	20% after 24 h (CUR) 55% after 24 h (DOX)	Colon carcinoma (C26) cells	Sesarman et al. (2019)
Cationic liposome/DOTAP, DOPE, C6 ceramide, and sodium cholate	142	0.242	+42.8	10	86.8	-	-	Melanoma (B16F10) cells	Jose et al. (2018)
Conventional liposome/composed by soybean phosphatidylcholine and cholesterol	126	0.057	-8.8	-	-	52.8 µM for Ishikawa cells 80.8 µM for HEC-1 cells	-	Human endometrial carcinoma (Ishikawa and HEC-1) cells	Xu et al. (2018)
Conventional liposome/cholesterol, DSPE-mPEG-2000 and DMPC	294	0.119	+10.8	3.42	93.4	0.62 µM	74% after 24 h	Human liver cancer (HepG2) cells	Cheng et al. (2018)
Hyaluronic acid coating liposome/cholesterol, DMPC, DMPG, DSPE, and DSPE-PEG (2000) Abbr.: HA-CUR-LSs	236	0.232	-36.8	13.2	66	10.9 µM (HA-CUR-LSs) 14.86 µM (CUR-LSs, *i.e.*, non-targeted LSs) 23.88 µ (free CUR)	60% after 48 h 95% after 144 h	Leukemia (K562, KG-1, and MV4-11) cells	Sun et al. (2017)

Type of liposomes systems/Composition	Size (nm)	PDI	ζ potential (mV)	%DL	%EE	IC_{50}	Release results	Cell lines evaluated	References
						(All for for KG-1 cells)			
Conventional liposome/caldarchaeol and calditoglycerocaldarchaeol	211	0.290	-22.6	3.0	83.5	16.1 µM (at 3.2 J/cm²) for SK-OV-3 cells	-	Human ovarian adenocarcinoma (SK-OV-3) cells and primary human coronary artery endothelial (PCS-100-020™) cells	Duse et al. (2017)
PEGylated coating liposome/phosphatidyl-choline, DOTAP, DSPE-mPEG-2000, and cholesterol	250	0.200	+7.0	9.09 (CUR) 5.9 (PTX)	99.9 (CUR) 99 (PTX)	4 µg/mL (CUR free) 12 µg/mL (PTX free) both for MCF 7 cells 1 µg/mL (CUR free) 5 µg/mL (PTX free) both for B16F10 cells	35% after 24 h	Human breast cancer (MCF 7) cells and mouse melanoma (B16F10) cells	Ruttala and Ko (2015)
Cationic liposome/soybean lecithin, Montanov82®, and DDAB (Abbr.: CUR-LSD) or soybean lecithin, cholesterol, and DDAB (Abbr.: CUR-LCD)	252 (CUR-LSD) 219 (CUR-LCD)	0.270 (CUR-LSD) 0.280 (CUR-LCD)	+28.8 (CUR-LSD) +27.7 (CUR-LCD)	0.9 (CUR-LSD) 1.8 (CUR-LCD)	34.7 (CUR-LSD) 68.9 (CUR-LCD)	21 µM for HeLa 16 µM for SiHa both for CUR free	64.6% (CUR-LSD) 80.3% (CUR-LCD) both after 48 h	HPV type 18 positive (HeLa) cells and Human cervical tumor (SiHa) cells	Saengkrit et al. (2014)

"-" this parameter was not reported by the authors;

Abbr.: Abbreviation of the formulation used by the authors;

DMPC: Dimyristoylphosphatidylcholine; DMPG: 1,2-Dimyristoyl-sn-glycero-3-phosphoglycerol, sodium salt; DOTAP: 1,2-dioleoyloxy-3-(trimethylammonium) propane; DPPC: Dipalmitoylphosphatidylcholine; DSPE: 1,2-distearoyl-sn-glycero-3-phospho-rac-glycero; DSPE-PEG (2000): Amine 1,2-distearoyl-sn-glycero-3-phosphoethanolamine-N-[amino(polyethylene glycol)-2000]; PTX: paclitaxel; and DOX: doxorubicin.

4.3 Niosomes

Nonionic surfactant vesicles, also known as niosomes (NIOs) are colloidal particles formed from the self-assembly of nonionic surfactants with or without cholesterol moieties in aqueous media, which results in a microscopic lamellar bilayer structure. The schematic representation NIOs structure is given in Figure 4. Structurally, NIOs are similar to liposomes and polymersomes, nanostructures that consist of a bilayer composed of phospholipids or copolymers, respectively. However, NIOs high chemical stability and economy make them superior to liposomes (Ashutosh et al., 2012). NIOs are microscopic lamellar structures (10 to 1,000 nm) which amphiphilic nature allows the entrapment of hydrophilic drugs in the core cavity and hydrophobic drugs in the non-polar region present within the bilayer (Ashutosh et al., 2012).
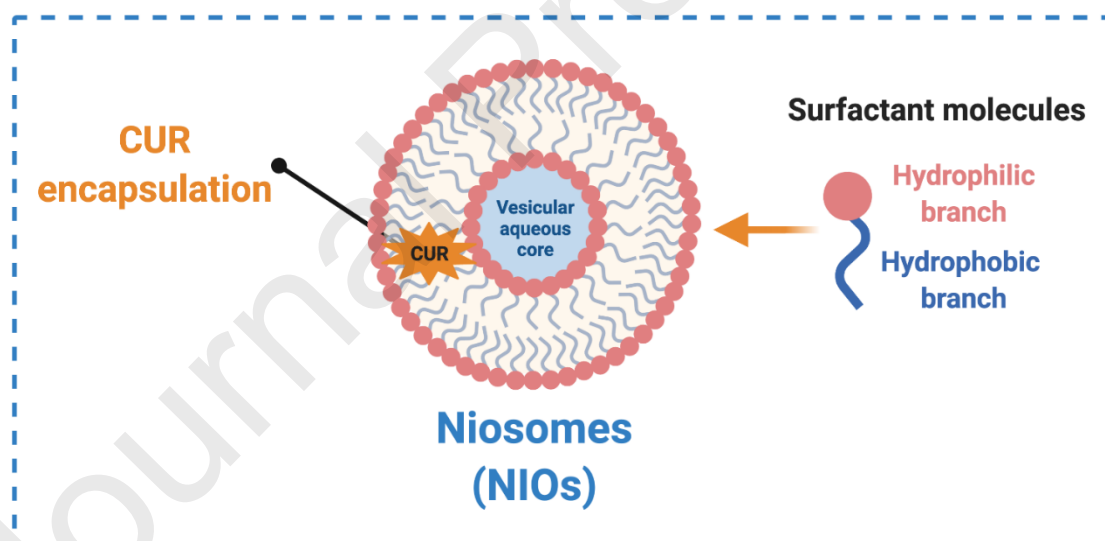

Figure 4. Schematic representation of niosomes (NIOs). NIOs are vesicles composed mainly of hydrated nonionic surfactants (such as series of Brijs, Spans, and Tweens), in many cases, added of cholesterol or its derivatives, based on Moghassemi and Hadjizadeh (2014).

NIOs are emerging in the DDS area due to their salient features such as biodegradability, biocompatibility, chemical stability, low production cost, low

toxicity, and easy storage and handling. Therefore, NIOs have been evaluated as carriers to deliver a vast number of anticancer drugs, genes, antigens, and other bioactive compounds (Bagheri et al., 2014).

Seleci et al. (2017) encapsulated DOX and CUR in polyethylene glycolated NIOs (PEGNIO). This research group employed the thin-film hydration method. To obtain high cellular internalization, PEGNIO surface was conjugated with a penetrating peptide (tLyp-1). The empty PEGNIO was 150 nm, while after co-encapsulation of the two drugs, the diameter obtained was 144 nm. The tLyp-1 peptide conjugation efficiency was 23.9%, and it did not change the formulations' size considerably since the PDI values ranged from 0.140 to 0.175. For CUR and DOX, the %*DL* was 32.6 and 23.3%, respectively. Within 32 h the release profiles of CUR and DOX at acidic pH (5.6) was 62 and 74%, respectively; and at physiological pH (7.4), the release values were 36 and 68%, respectively. The IC_{50} values were calculated to be 0.96, 0.90, and 0.76 µg/mL for DOX–CUR, PEGNIO/DOX-CUR and PEGNIO/DOX-CUR/tLyp-1, respectively. In both combinatory studies (*i.e.*, CUR and DOX), the results indicated that NIOs are a promising DDS for hydrophobic and hydrophilic drugs together and showed that the use of functionalized NIOs could increase drugs cytotoxicity against cancer cells.

In another study, Sharma et al. (2015) also investigated CUR and DOX encapsulation in NIOs and their release. These authors used the film hydration method to prepare NIOs by amphiphilic self-assembly of Tween-80 and cholesterol. The NIOs size and ζ potential values were 220 nm and -24 mV, respectively. Regarding the molecules' distribution, DOX hydrochloride (DOX·HCl) was encapsulated in the aqueous inner due to its hydrophilic

character, while CUR was encapsulated in the outer lipid bilayer because of its hydrophobicity. The %EE achieved for CUR and DOX was approximately 90 and 25%, respectively. The release profile showed that 79% of DOX is released within two days, followed by 70% CUR up to 1 week. The IC_{50} value of dual drug-loaded NIOs against HeLa cell lines was 1.8 μg/mL, which increased to 2.7 and 7.2 μg/mL for free DOX and CUR, respectively.

According to Puvvada et al. (2013), NIOs can be used in DDS as a substitute for liposomes, showing enhanced stability and biocompatibility. In this study, the group obtained NIOs for CUR encapsulation using poly (ethylene glycol) methyl ether acrylate (PEGMEA480) conjugated with cysteine (PEG-Cys). The average size of nanoformulations without (PEG-Cys-NIO) and with CUR (PEG-Cys-NIO-CUR) was found to be in the range of 160 to 185 nm and 160 to 210 nm, respectively. The cytotoxicity of both nanoformulations in cultured human breast cancer cell line (MCF7) showed that 30% cell viability was achieved with 40 μM of free CUR, while 25 μM of PEG-Cys-NIO-CUR was needed to achieve the same percentage of cell viability. Further, the group observed that free CUR showed an IC_{50} of 27 μM, whereas PEG-Cys-NIO-CUR IC_{50} was of 17 μM after 24 h of treatment.

Table 4 summarizes the main studies that address the preparation of CUR-NIOs nanoformulations for cancer therapy. The works found and highlighted by us, demonstrate that these nanoformulations are a promising therapeutic strategy against different types of cancer cells, such as human glioblastoma, ovarian cancer therapy, human breast cancer, and cervical carcinoma, among others. The NIOs size displayed values of 84 to 220 nm, these Ns were relatively monodisperse and stable. The IC_{50} values found for the CUR-

NIOs formulation have shown that less drug concentration (including when CUR is administered in combination with another drug, *e.g.*, DOX and PTX) can be administered to achieve the same cytotoxic effect regarding to free CUR, this effect is an advantage because it can generate a considerably reduction of side effects in cancer therapy, according to Table 4. Overall, NIOs seem to be an interesting DDS to suppress CUR degradation level compared to the conventional surfactants forming normal micelles. The rigidity of the NIO membrane, due to the presence of cholesterol moieties in the niosomal bilayer, increases the level of interaction between CUR and the oxyethylene units of nonionic surfactants molecules (*e.g.*, Tween-20 or Tween-80), while in normal micelles this type of interaction is not so strong because of the higher water accessibility on the hydration layer (Mandal et al., 2013). Other important observation related to NIOs is that the metabolic fate can be difficult to express, since some compounds used may not be biodegradable.

Table 4. Summary of curcumin-loaded niosomes (NIOs) approach for cancer therapy reported in the literature over the past 10 years. PDI, %*EE*, and *IC*$_{50}$ correspond to polydispersity index, efficiency of encapsulation, and the half-maximal inhibitory concentration, respectively.

Type of niosomes systems/Composition	Size (nm)	PDI	ζ potential (mV)	%*EE*	*IC*$_{50}$	Release results	Cell lines evaluated	References
Cationic PEGylated niosomal formulations containing Tween-60:cholesterol:DOTAP:DSPE-mPEG with combination of paclitaxel (PTX) and CUR	~90	-	+15	~100% for both drugs	Against MCF-7 cells: Free solution 44.6 µg/mL (CUR) 13.54 µg/mL (PTX) 8.36 µg/mL (CUR + PTX) Niosome solution 14.9 µg/mL (CUR) 3.73 µg/ml (PTX) 1.57 µg/mL (CUR + PTX) Against MCF-10A cells: Free solution 76.7 µg/mL (CUR) 30.7 µg/mL (PTX) 22.2 µg/mL (CUR + PTX) Niosome solution 64.2 µg/mL (CUR) 20.5 µg/ml (PTX) 8.8 µg/mL (CUR + PTX)	25% (12 h) 26% (24 h) 29.93% (72 h) (CUR at pH 7.4) 17% (12 h) 19% (24 h) 28.16% (72 h) (PTX at pH 7.4)	Human breast cancer (MCF-7) cells Human mammary epithelial (MCF-10A) cells	Alemi et al. (2018)
Polyethylene glycolated niosomes composed by Span-60, cholesterol, and DSPE-PEG (2000) maleimide conjugated with penetrating peptide (tLyp-1) **Abbr.: PEGNIO DOX-CUR-tLyp-1**	144 – 150	0.140 – 0.175	-	31.2% (CUR) 22% (DOX) (both for PEGNIO DOX-CUR-tLyp-1) 32.6% (CUR) 23.3% (DOX) (both for PEGNIO DOX-CUR)	0.76 µg/mL (PEGNIO DOX-CUR-tLyp-1) 0.90 µg/mL (PEGNIO DOX-CUR) 0.96 µg/mL (free DOX+CUR)	~36% after 12 h ~40% after 24 h ~62% after 32 h (CUR at pH 5.6) ~15% after 12 h ~35% after 24 h ~36% after 32 h (CUR at pH 7.4) ~60% after 12 h ~62% after 24 h ~74% after 32 h (DOX at pH 5.6) ~48% after 12 h	Human glioblastoma (U87) cells	Seleci et al. (2017)

	Size (nm)	PDI	Zeta potential (mV)	Encapsulation efficiency	IC50 / concentration	Drug release	Cell line	Reference
						~50% after 24 h ~68% after 32 h (DOX at pH 7.4)		
Combination of nonionic surfactants (Span-80, Tween-80, and Poloxamer-188) **Abbr.: CUR-NIO**	84	-	-25 – -20	92.3	-	45% after 6 h 80% after 24 h	Ovarian cancer (A2780) cells	Xu et al. (2016)
Nonionic surfactant Tween-80 and cholesterol with CUR + DOX encapsulated	220	0.265	-24	90% (CUR) 25% (DOX)	1.8 µg/mL (CUR+DOX) 7.2 µg/mL (free CUR) 2.7 µg/mL (free DOX)	~15% after 12 h ~25% after 24 h ~50% after 72 h (CUR at pH 7.4) ~15% after 12 h ~25% after 24 h ~55% after 72 h (CUR at pH 5.5) ~65% after 12 h ~65% after 24 h (DOX at pH 7.4) ~70% after 12 h ~80% after 24 h (DOX at pH 5.5)	HeLa (human cervical carcinoma) cells	Sharma et al. (2015)
Poly(ethylene glycol) methyl ether acrylate (PEGMEA-480) conjugated with cysteine **Abbr.: PEG-Cys-NIO-CUR**	160 – 210	-	~+6.5 (at pH 5.5) – ~-1.5 (at pH 7.0)	-	17 µM (24 h for PEG-Cys-NIO-CUR) 27 µM (24 h for free CUR)	~6% after 24 h ~8% after 48 h ~12% after 72 h (PEG-Cys-NIO-CUR at pH 7.0) ~30% after 24 h ~55% after 48 h ~70% after 72 h (PEG-Cys-NIO-CUR at pH 5.0)	Human breast cancer (MCF7) cells	Puvvada et al. (2013)

"-" this parameter was not reported by the authors;

Abbr.: Abbreviation of the formulation used by the authors;

DOX: doxorubicin hydrochloride; and (DSPE-PEG (2000) Maleimide): 1,2-distearoyl-*sn-glycero*-3-phosphoethanolamine-*N*-[maleimide (polyethylene glycol)-2000].

4.4 Nanoemulsions

Nanoemulsions (NEs) are biphasic dispersions, where one phase is dispersed in another phase [either oil-in-water (o/w) or water-in-oil (w/o) droplets] and stabilized by an emulsifier that reduces the interfacial tension between the two immiscible liquids (Jiang et al., 2020). NEs can present a mean droplet diameter between 20 to 200 nm (Figure 5), despite the lack of a current consensus on the upper limit (Choi and McClements 2020). Different emulsifiers such as biopolymers (*e.g.*, proteins and polysaccharides), phospholipids, surfactants (*e.g.*, Tween 80), and oils (*e.g.*, fats and essential oils) can be used to produce NEs (Choi and McClements, 2020; Pinheiro et al., 2016; Salvia-Trujillo et al., 2017).
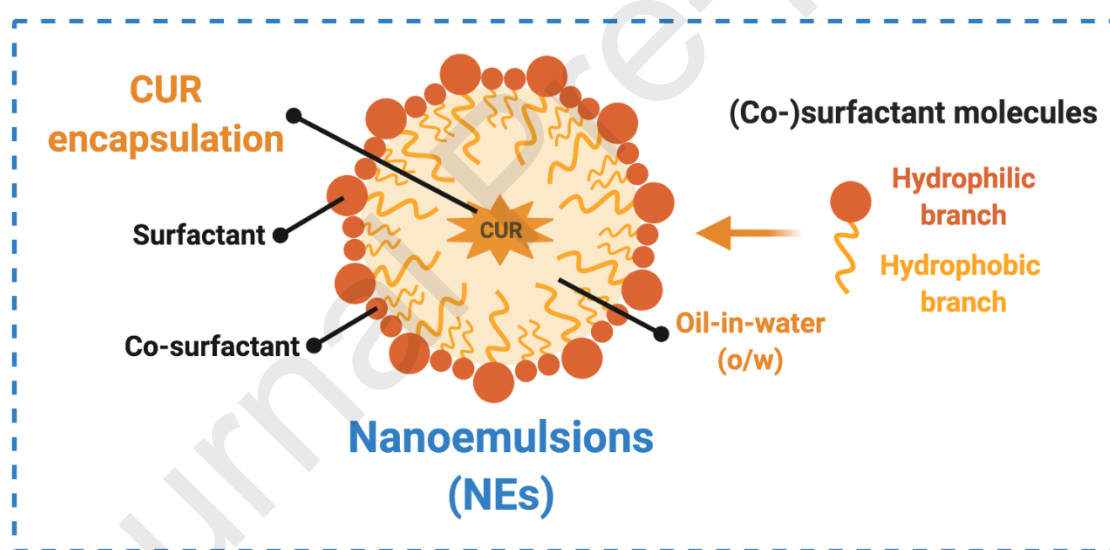

Figure 5. Schematic representation of oil-in-water (o/w) nanoemulsion (NEs) loaded with a hydrophobic drug, curcumin (CUR). NEs are formed by nano-scale droplets that contain an oil phase in the core dispersed in bulk aqueous phase (or vice-versa – w/o), with the help of an interfacially active compound (*i.e.*, surfactant). Based on Yoon et al. (2018) and Pachioni-Vasconcelos et al. (2015).

NEs have attracted significant attention due to their promising ability to encapsulate bioactive compounds for numerous applications in food,

pharmaceutical, and medical areas. Among the various nanoformulations, NEs are particularly suited for lipophilic compounds such as CUR to enhance their solubility and bioavailability. Besides, NE exhibits greater stability to gravitational separation and droplet aggregation than conventional emulsions (Choi and McClements, 2020). Therefore, several studies have been performed to show the prospect of using NE to create CUR delivery systems (Ahmad et al., 2019; Beloqui et al., 2016; Rafiee et al., 2018; Sari et al., 2015).

NEs must be thermodynamically stable and transparent. Nonetheless, the formation of NEs requires energy because they are non-equilibrium systems. Thus, CUR can be encapsulated in NEs using low or high energy methods. Low energy methods comprise the formation of oil droplets through the control of interfacial modification at the boundary between two immiscible phases and rely on the nature (*i.e*., molecular structure and solubility) of the molecules existing in the solution (Rafiee et al., 2018). On the other hand, high energy methods rely on high disruptive forces that physically break the oil droplets into fine droplets dispersed within the aqueous phase (McClements and Rao, 2011; Salvia-Trujillo et al., 2017). Usually, low energy methods are more efficient in producing smaller emulsions, but high energy methods have some advantages: *e.g*., the need for lower levels of emulsifiers and scale-up simplicity.

Some *in vitro* and *in vivo* research works have been conducted to assess the therapeutic performances (*e.g*., anticarcinogenicity), biological efficacy, and safety profile of NEs incorporating CUR. Studies have also shown that CUR encapsulated in NEs improved its anticancer effect compared with free CUR. For instance, Nikolic et al. (2020) developed low-energy NEs stabilized by polysorbate 80 and soybean lecithin as delivery systems for CUR and assessed

their therapeutic performance and safety profile. CUR-NE had a mean size diameter of <150 nm with a PDI ranging from 0.156 to 0.175. Cytotoxicity tests demonstrated that CUR-loaded NE possessed significant cytotoxic activity towards HeLa cell line (IC_{50} = 22.89 μg/mL) and human malignant melanoma (Fem-x cell line, IC_{50} = 37.87 μg/mL). On the other hand, free CUR presented IC_{50} values of 7.77 and 20.64 μg/mL for HeLa and Fem-x cell lines, respectively. The authors also stated that encapsulation raised CUR-NE safety profile compared to free CUR, the IC_{50} values towards normal lung fibroblast (MRC-5) cell line for CUR-NE and free CUR were 67.72 and 26.97 μg/mL, respectively.

In another study, CUR-o/w-NE prepared with Miglyol 812 (as oil), Epikuron 145 V (as surfactant), ethanol, and acetone by spontaneous nanoemulsification method showed anticancer efficacy (Guerrero et al., 2018). The average size, PDI, and ζ potential of the CUR-loaded NE were in the range of 195 to 217 nm, <0.200 and -30 to -36 mV, respectively. The %*EE* and %*DL* of CUR in the NE were 95 and 2.1%, respectively. Cell viability following treatment with CUR-loaded NE was assessed in various cancer cell lines, namely human gastric adenocarcinoma (AGS), colorectal adenocarcinoma (HT29-ATCC), cells derived from HT29-ATCC with elevated metastatic potential (HT29-US), human mammary gland adenocarcinoma (MDA-MB-231), and murine melanoma (B16F10). The observed IC_{50} values were 24, 26.2, 75.7, and 84.6 μM for AGS, MDA-MB-231, HT29-US, and HT29-ATCC cells, respectively, which indicated that this nanoformulation reduced cancer cell proliferation.

Other CUR-NE were developed using soy phospholipids (Lipoid S100), and surfactant poloxamer 188, and their effect as a potential natural photosensitizing drug in PDT for breast cancer (MCF-7 cell line) was studied

(Machado et al., 2019). The mean size diameter, PDI, and ζ potential of the CUR-NE were 199 nm, 0.179, and -46.3 mV, respectively. The results showed that the application of CUR-NE in PDT resulted in a desirable phototoxic effect (cell viability reduce to 57%) and increased reactive oxygen species generation in MCF-7 breast cancer cell line. In another study, CUR was formulated into o/w NE obtained with black pepper oil (oil phase) and Tween 80 (surfactant) at 1:9 ratio, and the *in vitro* cytotoxic effect of these NEs was assessed in Neuro2A cells (a fast-growing mouse neuroblastoma cell line) (Moghaddasi et al., 2018). CUR-NE were obtained with a mean particle size of 25.0 nm, PDI of 0.286, and ζ potential of -9.61 mV. Cytotoxicity was detected in the treated Neuro2A cells when CUR-NE were applied up to 15.63 µg/mL. The authors suggested that this CUR-NE could be potentially used as a cancer treatment.

Table 5 summarizes the most significant studies published during the last 10 years, regarding CUR-NEs delivery systems for cancer therapy. The CUR-NEs size showed values from ~34 to 202 nm, the values of PDI and zeta potential varied of 0.129 to 0.510, and -42 to -8.5 mV, respectively. In general aspects, CUR-NEs showed a good controlled and sustained release, as can be seen in Table 5. Interestingly, NEs can enable new delivery routes, for example, for the oral CUR delivery. In this case, Shukla et al. (2017) showed that CUR-NEs improved anticancer activity, as highlighted by this group this effect could be related to the enhanced oral bioavailability of CUR from NEs formulation. In addition, the mentioned researches demonstrate the potential of using NE to create CUR delivery systems with anticancer potential. Results obtained from the literature provide a basic knowledge of the cytotoxicity of NE on various cell types and can be used as a basis for future animal experiments.

Table 5. Summary of curcumin-loaded nanoemulsions (NEs) approach for cancer therapy reported in the literature over the past 10 years. PDI and IC_{50} correspond to polydispersity index, and the half-maximal inhibitory concentration, respectively.

Type of nanoemulsions systems/Composition	Size (nm)	PDI	ζ potential (mV)	IC_{50}	Release results	Cell lines evaluated	References
o/w NE: CUR, MCT oil, soy lecithin, Tween 80, and water	197 (with Tween 80) 202 (with lecithin)	0.200 – 0.300	-	-	-	Mouse fibroblasts (NIH3T3) cells Rat heart myoblasts (H9C2) cells Human hepatoblastoma (HepG2) cells Human endothelial progenitor (hEPC) cells Human cardiac progenitor (hCPC) cells	Yoon et al. (2018)
SNEDDS of CUR-phospholipid complex: CUR, phospholipid (L-α-phosphatidylcholine from egg yolk), castor oil, Tween 80, and PEG 400	83	0.150	-16	8.1 μM (CUR suspension) 7 μM (CUR-phospholipid complex) 4.3 μM (CUR-SNEDDS)	~5% of CUR after 2 h in SGF, pH 1.2 and ~30% of CUR after 24 h in SIF, pH 6.8 (CUR suspension) ~10% of CUR after 2 h in SGF, pH 1.2 and ~40% of CUR after 24 h in SIF, pH 6.8 (CUR-phospholipid complex) ~15% of CUR after 2 h in SGF, pH 1.2 and 93.1% of CUR after 24 h in SIF, pH 6.8 (CUR-SNEDDS)	Human breast cancer (MDA-MB-231) cells	Shukla et al. (2017)

Type of nanoemulsions systems/Composition	Size (nm)	PDI	ζ potential (mV)	IC_{50}	Release results	Cell lines evaluated	References
o/w NE: **CUR, MCT, cremophor RH 40, and glycerol**	34.54	0.129	-8.54	-	30% of CUR was released from NE at 37°C after 12 h incubation	Human prostatic carcinoma (PC3) cells	Guan et al. (2017)
w/o NE based lipid nanosystems: **CUR, ethyl oleate, water, CEL 35, PEG 400, glycerin monostearate, Lipoid S 75, and Tween 80**	121	-	-42	15 μM after 24 h (15.59%) 12.5 μM after 48 h (23.22%) 9 μM after 72 h (41.10%)	~70% after 170 h in pH 1.2 HCl solution (containing 0.5% SDS and 20% ethanol) and in pH 6.8 PBS ~70% after 170 h at pH 6.8 (PBS)	Human lung cancer (A549) cells	Wan et al. (2016)
Lipid NE: **CUR, soybean oil, HEPC from egg yolk, Tween 80, and HCO-60**	47.9 – 77.8	0.220 – 0.510	-	22.2 μM (B16F10) 53.7 μM (K562) 30.3 μM (Molt4) 35.8 μM (U937) 23.5 μM (HL-60)	25% (in human serum containing PBS at pH 7.4) 1.4% (in PBS alone) Both after 72 h	Leukemic cell lines [promyelocytic leukemia (HL-60), chronic myelocytic leukemia (K562), lymphoblastic leukemia (Molt4), and monocytic leukemia (U937)] and mouse melanoma cell line (B16F10)	Anuchapreeda et al. (2012)

"-" this parameter was not reported by the authors;

CEL 35: Cremophor EL 35; HCO-60: Cremophor-HR60; HEPC: hydrogenated L-α-phosphatidylcholine; MCT: medium chain triglyceride; o/w: oil-in-water; PBS: Phosphate-buffered saline; PEG: polyethylene glycol; SDS: sodium dodecyl sulfate; SIF: simulated intestinal fluid; SGF: simulated gastric fluid; SNEDDS: self-nanoemulsifying drug delivery system; and w/o: water-in-oil.

4.5 Hydrogels

Hydrogels (HGs) began to be explored in 1960, although the origin of the term "hydrogel" appeared in 1894 and was first marketed in 1949 with the application of poly(vinyl alcohol) cross-linked with formaldehyde for biomedical implants (Cascone and Lamberti, 2020; Wichterle and Lím, 1960). After long years of industrial applications, HGs have been widely studied because of their three-dimensional networks, non-solubility in water at a physiological temperature or pH, noticeable swellability in aqueous media, and porosity formed by physical (*e.g.*, hydrogen bonds, entanglement of chains, ionic gelation, and van der Waals interactions) or chemical (simple monomers reaction - covalent bonds) cross-linking of molecules, as depicted in Figure 6. These characteristics allow water absorption and retention in the interstitial spaces between chains, which increase their volume and potentiate a multitude of different mechanical behaviours, making them an interesting and potentially intelligent (*i.e.*, reactive to external stimuli) material to be used as controlled release systems of bioactive molecules (Amiriana et al., 2021; Pettinelli et al., 2020).
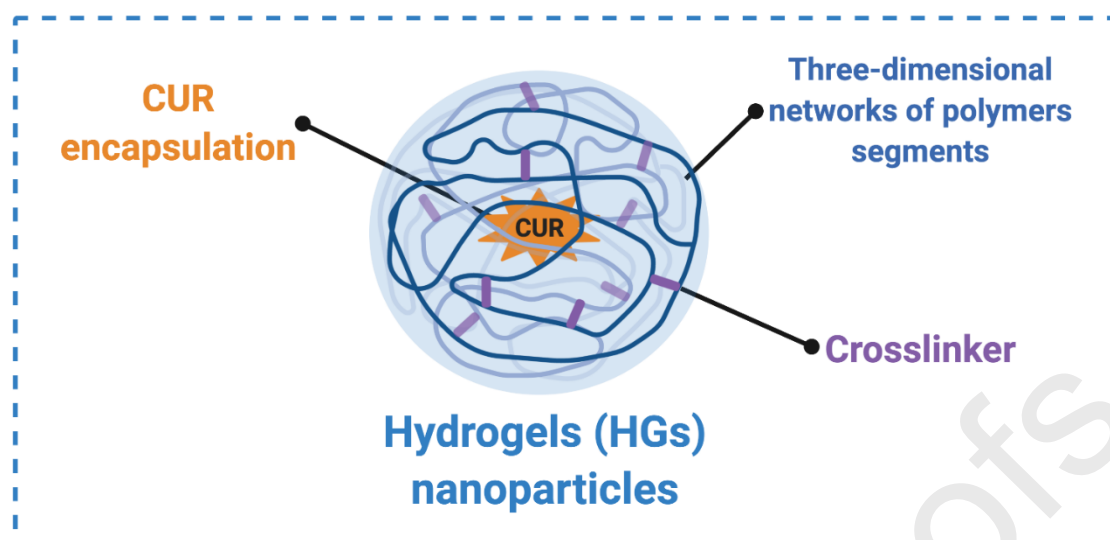
Figure 6. Schematic representation of hydrogels nanoparticles (HGs). Purple rectangle: crosslinker (hydrophobic interaction, hydrogen bond, electrostatic interaction, coordination, host-guest interaction). Blue lines: polymer segments, based on Pachioni-Vasconcelos et al. (2015).

Despite their highly hydrophilic nature, HGs allow the incorporation of hydrophobic compounds such as CUR, into the gel matrix, encapsulating and protecting those until they reach a specific target within the human body (*e.g.*, mouth, stomach, liver, prostate, small intestine, and colon). This result in increased drugs bioavailability, reduction of side effects, control of kinetic release profiles, easy clinical administration, and low costs (Alavi et al., 2018; Feng et al., 2020). Nowadays, HGs are designed to be oral (most commonly used), transdermal, vaginal, and ocular administered. More specifically, HGs when injected present a low viscosity liquid and then cross-linked into viscoelastic gels through an exposure to different stimuli, specific physiological changes or external conditions (*e.g.*, radiation, enzymes, salt, and temperature), while protecting cells and bioactives, such as CUR, from the hostile environment due to *e.g.* stomach acidity, enzymes, and immune system activity (Abdel-Wahhab et

al., 2019; Cascone and Lamberti, 2020; Pushpalatha et al., 2019; Songkroh et al., 2015).

Polysaccharide-based HGs have been intensively studied as site-specific delivery agents of CUR because their physicochemical and biological properties (*e.g.*, biodegradability, biocompatibility, hydrophilicity, non-toxicity, water-retaining capacity, and mechanical stability) provide unique characteristics for medical applications. However, some setbacks were found due to inadequate formulations, especially those based on one single biopolymer that often cannot show efficient CUR loading and targeted release. For this reason, one or more polysaccharides and mechanisms may be used to increase the entrapment efficiency and prevent a precocious disintegration, ensuring the release at the expected target, *i.e*., tumour cells (Feng et al., 2020; Liu et al., 2020; Mahmoud and Marzok, 2020). Additionally, the polysaccharide HGs' tuneable structure and network morphology offer interesting and adaptable physical properties, such as density, refractive index, and rheological properties, when exposed to varying environmental conditions (Abaee et al., 2017). On the other hand, mixtures of polysaccharide-based structures and proteins have also been widely studied (Table 6) to protect and deliver CUR to the final target. Proteins carry a high nutritional value, antioxidant capacity, functional properties, amphiphilic nature, biocompatibility, biodegradability, low toxicity, and contribute to the chemical and photo-stability of CUR (Alavi et al., 2018).

Colon-targeted HGs as vehicles of drugs such as CUR have emerged due to increasing concerns with colon health (Feng et al., 2020). Alavi et al. (2018) designed an orally administrated colon-targeted HG delivery system based on whey-protein aggregates (WPA)/k-carrageenan (KC) (named as WPA/KC HG)

for CUR encapsulation to battle cancer or inflammatory bowel diseases. This nanoformulation showed an %*EE* above 92% and a water holding capacity above 96%. This work confirmed the importance of adding a polysaccharide to the protein-based HG once the physical stability of CUR was highly improved with the KC addition. Besides that, WPA/KC HG nanoformulation increased the CUR delivery efficiency in the colon, as 87% of the loaded CUR were delivered to the colon where colon microorganisms could degrade the complex WPA/KC HG network. Additionally, only 3.5% of WPA/KC HG was degraded after the gastrointestinal digestion.

Table 6 summarizes the main studies that address the preparation of CUR-HGs nanoformulations for cancer therapy. The HGs size displayed values of 188 and 490 nm, with zeta potential values ranging from -34.5 to -5.8 mV, according to Table 6. In general, the number of studies with HGs in cancer therapy is still low, and therefore, there is an enormous potential to be investigated. In this sense, despite the widespread use of HGs as delivery vehicles for bioactive compounds, in the particular case of CUR, specifically, there are still many possibilities to be explored to improve their performance and specificity. Additionally, smart HGs can respond to external stimuli (*i.e.*, light, pH, ultrasound, and temperature), allowing *in situ* gelation, and a more sustained and controlled drug release. The studies highlighted by us in Table 6 have shown that these Ns release CUR in a controlled and sustained manner, employing materials/biomaterials with biodegradable and biocompatible characteristics, which is an advantage as a DDS.

Table 6. Summary of curcumin-loaded hydrogels (HGs) approach for cancer therapy reported in the literature over the past 10 years. IC_{50} corresponds to the half-maximal inhibitory concentration, respectively.

Type of hydrogels systems/Composition	Size (nm)	ζ potential (mV)	IC_{50}	Release results	Cell lines evaluated	References
Chitosan/β-sodium glycerophosphate	-	-	-	~40% after 48 h	Prostate cancer (CWR22RV1) cell	Zhou et al. (2019)
Cyclodextrin-based nanosponges (CDN)	490.9	-34.5	10.11 µg/mL	CDN enhanced the CUR release 10 times more than free CUR after 8 h	Breast cancer (MCF-7) cell	Pushpalatha et al. (2019)
Chitosan/Chondroitin sulfate conjugated with silver nanoparticles (AgNPs)	-	~-5.8*	91.5 µg/mL	~10 – 12% after 24 h	Colorectal cancer (Caco-2) cell	Freitas et al. (2020)
Gellan gum-based (GB)	-	-	-	3.26% after 4 h 30.94% after 24 h	Gastric cancers and ulcers	Mahmoud and Marzok (2020)
Cyclodextrin-based (CB)	-	-	702.27 mg/mL	The complexes of CUR inclusion resulted in a constant release kinetics, independently of the drug concentration (~100% after 4 h), appropriate for continuous release of bioactives to exert therapeutic effects	Melanoma (B16-F10) cell	Sun et al. (2014)
Thiolated chitosan/ poly(ethyleneglycol) diacrylate	-	-	-	~6% after 1 day 55% after 7 days both without addition of lysozyme ~45% after 1 day 85% after 7 days both with addition of lysozyme (0.75 g/g)	Human liver cancer (HepG2) cell	Ning et al. (2018)
Poly (ε-caprolactone-*co*-lactide)-*b*-poly (ethylene glycol)-*b*-poly (ε-caprolactone-*co*-lactide) (PCLA-PEG-PCLA) incorporating CUR-loaded polyethylene glycol-*b*-polylactide (mPEG-PLA)	188.6**	-15**	25.5 mg/Kg***	~24.5% for mPEG-PLA after 5 h 66.7% for mPEG-PLA after 240 h 14.5% for PCLA-PEG-PCLA-mPEG-PLA after 5 h 39% for PCLA-PEG-PCLA-mPEG-PLA after 240 h	Glioma tumor (C6) cell	Babaei et al. (2020)

"-" this parameter was not reported by the authors.

*AgNPs with CUR; **CUR-encapsulated mPEG-PLA nanopolymersomes (Poly-CUR); and ***Suppressed the tumor growth and the tumor volume of mice treated in comparison with the original tumor size.

4.6 Nanocomplexes

In this section, we will consider nanometric structures formed by one type of carrier molecule (protein or oligosaccharide), which interacts/aggregates with CUR by non-covalent interactions to form a nanoaggregate (or nanocomplexe), as depicted in Figure 7. In this sense, the most relevant nanocomplexes that enhance CUR solubility involves the use of cyclodextrins (CD). CDs are cyclic glucose polymers consisting of six (α-), seven (β-) or eight (γ-) units linked by α-(1,4) glycosidic bonds, which have an inner cavity that can bind hydrophobic molecules, forming stable hydrophilic complexes that enhances CUR water solubility (Table 7) and dissolution kinetics (Rocks et al., 2012; Ntoutoume et al., 2016). Noteworthy, CUR studies focus on solubility and inclusion characterization and rarely on measuring the diameter size. However, this measure is essential to characterize the aggregation state since particle size depends on concentration of CD, complexed drugs, and formulation excipients. In addition, particle size can change internalization pathways and targeting, again highlighting the need for better characterization of these complexes concerning their size profile (Zaman et al., 2017).
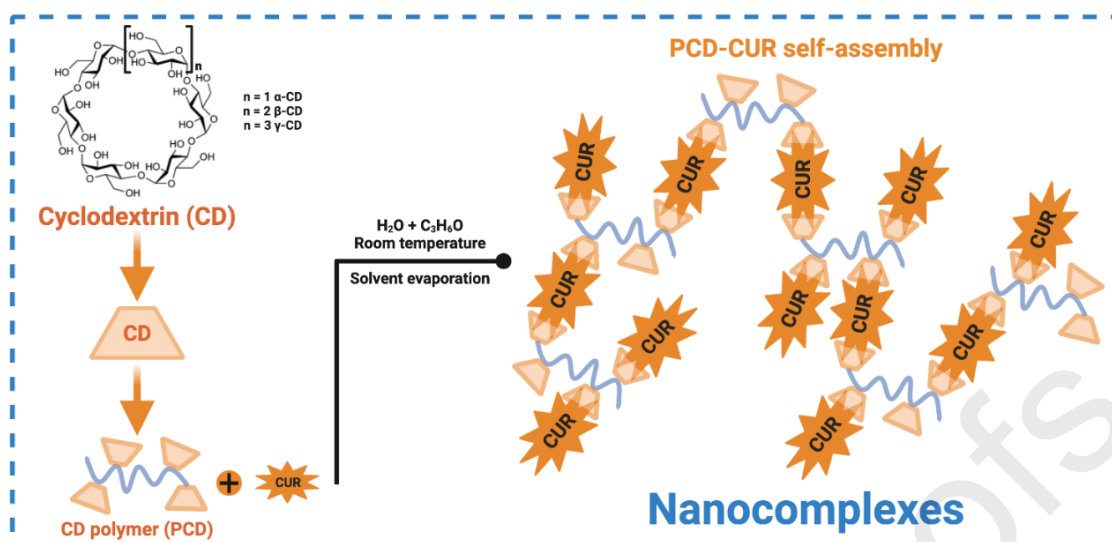
Figure 7. Schematic representation of polymeric β-cyclodextrin/curcumin (PCD/CUR) self-assembly through the inclusion complexation mechanism formation, based on Yallapu et al. (2010).

Table 7. Curcumin solubility in different cyclodextrins (CD).

CD type	Solubility (mM)	Reference
β-CD	~0.05 (20 mM CD)	
γ-CD	~0.15 (20 mM CD)	Yadav et al. (2009)*
Hydroxypropyl-β-CD	~0.32 (20 mM CD)	
Methyl-β-CD	~0.51 (20 mM CD)	
β-CD	1.12 (60 mM CD)	Mangolim et al. (2014)**
Hydroxypropyl-γ-CD	1.98 (57 mM CD)	Singh et al. (2010)***
Hydroxypropyl-β-CD	0.27 (70 mM CD)	

*Solubility in aqueous solution. Values obtained from the phase solubility diagram of curcumin–CD complexes. **Solubility in aqueous solution. ***Solubility in phosphate buffer (0.1 M, ionic strength 0.3) pH 6.0.

CUR-β-CD complexes (%*DL* of 15%) were shown to increase molecule solubility and antitumor activity against lung tumor provoked by H22 cells in mice. The enhancement elucidated *in vitro* (A549 cells) was related to improved cellular uptake and modified-release kinetics (Zhang et al., 2016). Polymeric β-CD were also complexed with CUR and formed NSs of 250 nm in higher CUR

45

concentrations, with a %*DL* of 23% (*i.e.*, 223.2 µg of CUR per mg of CD). It reached an 80-fold enhanced solubility and an improved *in vitro* stability at physiological pH conditions: after 72 h immersed in PBS buffer, almost 100% of free CUR precipitated, whereas only 11% of the complexed CUR precipitated. As for monomeric β-CDs, the polymeric complex showed higher antitumor and cytotoxic activity than free CUR in prostate cancer cells. The *IC*$_{50}$ values for prostate cancer cell lines C4-2, DU145, and PC3 were 19.6, 19.25, and 19.4×10^{-6} M for free CUR and 12.5, 15.9, and 16.1×10^{-6} M for CUR complexed with β-CD, respectively (Yallapu et al., 2010).

CUR-Hydroxypropyl-β-CD (HP-β-CD) complexes showed an even higher solubility (202-fold) and a modified dissolution profile of 50% release in 6 h, with 100% of CUR dissolved in 12 h. In addition, complexation increased the biological effects, demonstrated by greater antiangiogenic effects than free CUR in chick chorioallantoic membrane model and by the decrease in the disease' extent and severity in a rat colitis model (histopathological outcomes) (Yadav et al., 2009).

Rocks et al. (2012) treated implanted tumors in mice with CUR-hydroxypropyl-γ-cyclodextrin (CUR-HP-γ-CD)-gemcitabine complexes, as the treatment inhibited lung tumor growth. The association of CUR-HP-γ-CD and gemcitabine presented a 2-fold reduction of cell proliferation in mice lung tumors compared to the vehicle or non-soluble CUR treatments. However, there was no report of physicochemical characteristics of the formulation.

Concerning other nanoaggregates, the stability and aqueous solubility of CUR was significantly improved in the presence of proteins, which are folded in nanostructured particles, as result this molecule is encapsulated. Some of these proteins are not yet widely employed in cancer therapy, however, some of them

have been used to increase CUR solubility and stability. In particular, CUR formulations with pea and zein proteins have been studied, showing increased solubility, photo and thermal stability. The results generated have been interesting and have shown great potential for their use in the near future. Thus, for the interested reader, we would like to recommend some articles on the topic: Guo et al. (2021); Liu et al. (2018); Rafiee et al. (2018); Vijaian et al. (2021); Wang et al. (2019).

Moreover, as in most CDs studies, protein-CUR complexes generally lack physicochemical measurements such as size, particle charge, or drug release kinetics. For instance, CUR-casein complexes do not present these physicochemical indications. However, the work showed that complexation increased the half-life of CUR in Tris-HCl buffer (pH 7.2) approximately 39-fold (*i.e.*, from 8.8 min to 340 min), and degradation rates decreased from 90% after 30 min to 55% after 6 h of incubation (Sneharani et al., 2009). CUR combined with BSA was also protected from degradation, showing only 24% degradation after 1,000 min in sodium phosphate buffer (pH 7.0), whereas free CUR decomposes by 53% (Yang et al., 2013).

Chen et al. (2014) encapsulated CUR in the inner cavity of recombinant human H-chain ferritin presented the smallest size of measured CUR-protein complexes (12 nm), but low %*EE* (14.7%), and %*DL* of 1.07%. These nanoparticles increase CUR water solubility about 492-fold and improved its photo-stability: 69% of free CUR degraded after 50 min when exposed to an incandescent lamp, whereas only 11% of complexed CUR was degraded.

Protein complexes may perform better with surfactants like dextran, which diminish undesired aggregation. Yi et al. (2016) studied the effect of CUR coating

with α-lactalbumin or α-lactalbumin-dextran complex on its stability. The protein coating formed a nanocomplex of 63.5 nm (PDI of 0.108, ζ potential of -13.9 mV, and %*EE* of 97.5%), while CUR coated with α-lactalbumin and dextran showed a size of 68.1 nm (PDI of 0.161, ζ potential of -10.5 mV, and %*EE* of 98.8%). CUR coated with α-lactalbumin-dextran presented no changes in the mean particle diameters upon heating for 30 min (70, 80, and 90ºC) or when submitted to pH variations, performing better than the pure protein coating. However, both nanocomplexes exhibit less degradation in water dispersion after 4 h storage: 91.7% of CUR remained in α-lactalbumin complex, and 92.1% in α-lactalbumin-dextran conjugates, while only 24.8% was left when free CUR was used.

A study of CUR bonded in another globulin (β) presented the formation of bigger nanoparticles (142 nm) but also high %*EE* (>96%). CUR stability in 50 mM Tris-HCl buffer (pH 7.0) was increased by 6.7 times when in its complex form, and its water solubility was enhanced by ~20,800 times (Sneharani et al., 2010). Another high encapsulation formulation was CUR-soy protein complex (%*EE* of 96.8 to 99.1%, with %*DL* of 1.743 to 1.784 µg/mg of soy protein). The dried nanocomplex prepared with a protein concentration of 1.0% (w/v), improved the CUR water solubility about 1600-fold. The complex size was about 90 nm, and the ζ potential was between -10.95 and -13.20 mV.

Despite a few studies to date applied to cancer therapy, these results based on CUR in nanocomplexes may present promising DDS platforms for treatment of tumor cells. This approach is expected to be of wide applicability to this important class of Ns where CUR solubility is enhanced by CD and other excipients as well as to allow using a low-dose bioavailable CUR that is preferable to reduce potential side effects.

5. Final considerations

CUR has several interesting properties for medical applications, including antimicrobial, antioxidant, anti-inflammatory, and excellent antitumoral activity. However, it presents several drawbacks (*e.g.*, low solubility in water and instability), which challenge the creation of stable formulations for commercial medical products.

In the last 10 years, several research groups around the world have been proposing different nanocarriers to encapsulate CUR to improve its efficacy as a therapeutic agent against cancer. As shown in this review, CUR nanoformulations demonstrated superior therapeutic effects against cancer compared to the drug's free form. CUR interferes with the proliferation and survival of tumor cells, both directly and indirectly, due to its capacity to interact with various targets such as growth factors, DNA, RNA, transcription factors, and diverse biomolecules involved in cell signal transduction pathways.

As detailed previously, CUR has been encapsulated in micelles and liposomes for antitumoral use because of their interesting features such as high loading capacity, good stability, easy preparation, and low PDI values. These Ns types will probably persist in the future, mainly with responsive approaches to external stimuli (*e.g.*, pH, temperature, etc.). However, novel nanosystems can be designed and demonstrate better responses in cancer therapy. In this sense, we pointed out potential nanocarriers of different compositions with or without target ligands developed for the encapsulation and release of CUR, such as: epidermal growth factor (EGF)-conjugated chitosan NSs, mesoporous silica nanocarrier composed by chitosan, folate conjugated poly-D,L-lactic-*co*-glycolic

acid (PLGA) NSs, Gemini surfactants micelles, dendrosomes, nanosuspensions, solid lipid nanoparticles, polymeric nanoparticles, phytosomes, cubosomes, and inorganic nanoparticles. Besides the inherent advantages of Ns for encapsulation, some works mentioned in this review show that it is feasible to design them to deliver CUR to target sites through pH-responsive, thermo-responsive, and other methods, improving the delivery and, consequently, and diminishing side effects, illustrating how CUR nanoformulation can become more attractive in the future for antitumoral treatments.

Another important consideration is that in classical chemotherapy treatments, the combination of drugs with synergic effects is widely used, aiming at greater cellular death. Hence, CUR nanoformulations in cancer therapy were combined with other antineoplastic drugs, like doxorubicin, docetaxel, and paclitaxel. As highlighted before, this combination of antineoplastic drugs and CUR can improve antitumor effects and reduce dose-limiting toxicity. Additionally, combinations can overcome drug resistance that is common in classical chemotherapy. Thus, we also believe that the combination with other drugs will continue to be a strong trend for CUR nanoformulations.

Acknowledgements

(FCT) under the scope of the strategic funding of UIDB/04469/2020 unit and BioTecNorte operation (NORTE-01-0145-FEDER-000004) funded by the European Regional Development Fund under the scope of Norte2020 - Programa Operacional Regional do Norte. Our Figures were created with BioRender.

6. References

Abaee, A., Mohammadian, M., Jafari, S.M., 2017. Whey and soy protein-based hydrogels and nano-hydrogels as bioactive delivery systems. Trends Food Sci Technol. 70, 69–81. 10.1016/j.tifs.2017.10.011.

Abdel-Wahhab, M.A., Salman, A.S., Ibrahim, M.I.M., El-Kady, A.A., Abdel-Aziem, S.H., Hassan, N.S., Waly, A.I., 2016. Curcumin nanoparticles loaded hydrogels protects against aflatoxin B1-induced genotoxicity in rat liver. Food Chem Toxicol. 94, 159-171. doi: 10.1016/j.fct.2016.06.005.

Ahmad N., Ahmad R., Al-Qudaihi A., Alaseel S.E., Fita I.Z., Khalid M.S., Pottoo F.H., 2019. Preparation of a novel curcumin nanoemulsion by ultrasonication and its comparative effects in wound healing and the treatment of inflammation. RSC Advances. 9, 20192-20206. doi: 10.1039/c9ra03102b.

Akbar, M.U., Zia, K.M., Nazir, A., Iqbal, J., Ejaz, S.A., Akash, M. S. H., 2018. Pluronic-based mixed polymeric micelles enhance the therapeutic potential of curcumin. AAPS Pharm. Sci. Tech. 19, 2719–2739. doi: 10.1208/s12249-018-1098-9.

Alavi, F., Emam-Djomeh, Z., Yarmand, M.S., Salami, M., Momen, S., Moosavi-Movahedi, A.A., 2018. Cold gelation of curcumin loaded whey protein aggregates mixed with kcarrageenan: Impact of gel microstructure on the gastrointestinal fate of curcumin. Food Hydrocoll. 85, 267-280. doi: 10.1016/j.foodhyd.2018.07.012.

Alemi, A., Reza, J.Z., Haghiralsadat, F., Jaliani, H.Z., Karamallah M.H., Hosseini S.A., Karamallah S.H., 2018. Paclitaxel and curcumin coadministration in novel cationic PEGylated niosomal formulations exhibit enhanced synergistic antitumor efficacy. J. Nanobiotechnol. 16(1) 23-28. doi: 10.1186/s12951-018-0351-4.

Altunbas, A., Lee, S.J., Rajasekaran, S.A., Schneider, J.P, Pochan, D.J., 2011. Encapsulation of curcumin in self-assembling peptide hydrogels as injectable drug delivery vehicles. Biomaterials, 32, 5906-5914. doi: 10.1016/j.biomaterials.2011.04.069.

Alves, R.C., Fernandes, R.P., Fonseca-Santos, B., Victorelli, F.D., Chorilli, M., 2019. A critical review of the properties and analytical methods for the determination of curcumin in biological and pharmaceutical matrices. Critical

reviews in analytical chemistry, 49(2), 138-149. Doi: https://doi.org/10.1080/10408347.2018.1489216.

Al-Yousef, N., Shinwari, Z., Al-Shahrani, B., Al-Showimi, M., Al-Moghrabi, N., 2020. Curcumin induces re-expression of BRCA1 and suppression of γ synuclein by modulating DNA promoter methylation in breast cancer cell lines. Oncology reports. 43(3), 827-838. doi: 10.3892/or.2020.7473.

Amiriana, J., Zeng, Y., Shekh, M.I., Sharma, G., Stadler, F.J., Song, J., Du, B., Zhu, Y., 2021. *In-situ* crosslinked hydrogel based on amidated pectin/oxidized chitosan as potential wound dressing for skin repairing. Carbohydr. Polym. 251, 117005. doi: 10.1016/j.carbpol.2020.117005.

Anuchapreeda S., Fukumori Y., Okonogi S., Ichikawa H., 2012. Preparation of lipid nanoemulsions incorporating curcumin for cancer therapy. J Nanotech. 1-11. doi: 10.1155/2012/270383.

Babaei, M., Davoodi, J., Dehghan, R., Zahiri, M., Abnous, K., Taghdisi, S.M., Ramezani, M., Alibolandi, M., 2020. Thermosensitive composite hydrogel incorporated with curcumin-loaded nanopolymersomes for prolonged and localized treatment of glioma. J Drug Deliv Sci Tec. 59, 101885. doi: https://doi.org/10.1016/j.jddst.2020.101885.

Bagheri, A., Chu, B., Yaakob, H., 2014. Niosomal drug delivery systems: formulation, preparation and applications. World Applied Sciences Journal. 32 (8): 1671-1685, 2014. doi: 10.5829/idosi.wasj.2014.32.08.848.

Belcaro, G.; Hosoi, M.; Pellegrini, L.; Appendino, G.; Ippolito, E.; Ricci, A.; Togni, S., 2014. A controlled study of a lecithinized delivery system of curcumin (Meriva®) to alleviate the adverse effects of cancer treatment. Phytother Res. 28(3), 444-450. doi: https://doi.org/10.1002/ptr.5014.

Beloqui A., Memvanga P.B., Coco R., Reimondez-Troitiño S., Alhouayek M., Muccioli G.G., Alonso M.J., Csaba N., de la Fuente M., Préat V., 2016. A comparative study of curcumin-loaded lipid-based nanocarriers in the treatment of inflammatory bowel disease. Colloids Surf B Biointerfaces. 143, 327-335. doi: 10.1016/j.colsurfb.2016.03.038.

Cao, H., Yu, H., Feng, Y., Chen, L., Liang, F., 2017. Curcumin inhibits prostate cancer by targeting PGK1 in the FOXD3/miR-143 axis. Cancer Chemother Pharmacol. 79(5), 985-994. doi: 10.1007/s00280-017-3301-1.

Carvalho, D.D.M., Takeuchi, K.P., Geraldine, R.M., Moura, C.J.D., Torres, M.C.L., 2015. Production, solubility and antioxidant activity of curcumin nanosuspension. Food Sci Technol. 35(1), 115-119. doi: 10.1590/1678-457X.6515.

Cascone, S. and Lamberti, G., 2020. Hydrogel-based commercial products for biomedical applications: a review. Int J Pharm. 573, 118803. doi: 10.1016/j.ijpharm.2019.118803.

Chemspider. http://www.chemspider.com/Chemical-Structure.839564.html?rid=8b35c214-82ea-47b7-a0c7-fd1d81b878c2&page_num=0 (accessed 20 August 2020).

Chen, L., Bai, G., Yang, R., Zang, J., Zhou, T., Zhao, G., 2014. Encapsulation of curcumin in recombinant human H-chain ferritin increases its water-solubility and stability. Food Chem. 149, 307-12. doi: 10.1016/j.foodchem.2013.10.115.

Cheng Y., Zhao, P., Wu, S., Yang, T., Chen, Y., Zhang, X., 2018. Cisplatin and curcumin co-loaded nano-liposomes for the treatment of hepatocellular carcinoma. Int J Pharm. 545(1–2):261–73. doi: 10.1016/j.ijpharm.2018.05.007.

Choi, S.J., McClements, D.J., 2020. Nanoemulsions as delivery systems for lipophilic nutraceuticals: strategies for improving their formulation, stability, functionality and bioavailability. Food Sci Biotechnol. 29(2), 149-168. doi: 10.1007/s10068-019-00731-4.

Dai, J., Gu, L., Su, Y., Wang, Q., Zhao, Y., Chen, X., Deng, H., Li, W., Wang, G., Li, K., 2018. Inhibition of curcumin on influenza A virus infection and influenzal pneumonia via oxidative stress, TLR2/4, p38/JNK MAPK and NF-κB pathways. Int Immunopharmacol. 54, 177-187. doi: 10.1016/j.intimp.2017.11.009.

Damarla, S.R., Komma, R., Bhatnagar, U., Rajesh, N., Mulla, S.M.A., 2018. An evaluation of the genotoxicity and subchronic oral toxicity of synthetic curcumin. J Toxicology. e6872753 doi: 10.1155/2018/6872753.

Dasiram, J.D., Ganesan, R., Kannan, J., Kotteeswaran, V., Sivalingam, N., 2017. Curcumin inhibits growth potential by G1 cell cycle arrest and induces apoptosis in p53-mutated COLO 320DM human colon adenocarcinoma cells. Biomed Pharmacother. 86, 373-380. doi: 10.1016/j.biopha.2016.12.034.

Dei Cas, M., Ghidoni, R., 2019. Dietary curcumin: correlation between bioavailability and health potential. Nutrients. 11(9), 2147. doi: 10.3390/nu11092147.

Dhule, S.S., Penfornis, P., Frazier, T., Walker, R., Feldman, J., Tan, G., He, J., Alb, A., John, V., Pochampally, R., 2012. Curcumin-loaded γ-cyclodextrin liposomal nanoparticles as delivery vehicles for osteosarcoma. Nanomedicine. 8(4), 440-51. doi: 10.1016/j.nano.2011.07.011.

DrugBank. https://go.drugbank.com/drugs/DB11672 (accessed 15 September 2020).

Duse, L., Pinnapireddy, S.R, Strehlow B, Jedelská, J., Bakowsky, U., 2017. Low level LED photodynamic therapy using curcumin loaded tetraether liposomes. Eur J Pharm Biopharm. 126, 233–41. doi: 10.1016/j.ejpb.2017.10.005.

Edwards, R.L.; Luis, P.B.; Varuzza, P.V.; Joseph, A. I.; Presley, S.H.; Chaturvedi, R.; Schneider, C., 2017. The anti-Inflammatory activity of curcumin is mediated by its oxidative metabolites. J Biol Chem. 292(52), 21243-21252. doi: 10.1074/jbc.RA117.000123.

Epstein, J., Sanderson, I.R., Macdonald, T.T., 2010. Curcumin as a therapeutic agent: the evidence from *in vitro*, animal and human studies. Br J Nutr. 103(11), 1545-57. doi: 10.1017/S0007114509993667.

Feng, K., Wei, Y.-S., Hu, T.-G., Linhardt, R.J., Zong, M.-H., Wu, H., 2020. Colon-targeted delivery systems for nutraceuticals: A review of current vehicles, evaluation methods and future prospects. Trends Food Sci Tech.102, 203-220, doi: 10.1016/j.tifs.2020.05.019.

Feng, T., Wei, Y., Lee, R.J., Zhao, L., 2017. Liposomal curcumin and its application in cancer. Int J Nanomedicine. 12, 6027-6044. doi: 10.2147/IJN.S132434.

Freitas, C.F., Kimura, E., Rubira, A.F., Muniz, E.C., 2020. Curcumin and silver nanoparticles carried out from polysaccharide-based hydrogels improved the photodynamic properties of curcumin through metal-enhanced singlet oxygen effect. Mater Sci Eng C Mater. 112, 110853. doi: 10.1016/j.msec.2020.110853.

Garcia-Gomes, A.S., Curvelo, J.A.R., Soares, R.M.A., Ferreira-Pereira, A., 2012. Curcumin acts synergistically with fluconazole to sensitize a clinical isolate of Candida albicans showing a MDR phenotype. Medical Mycology. 50,26-32. doi:10.3109/13693786.2011.578156.

Gou, M., Men, K., Shi, H., Xiang, M., Zhang, J., Song, J., Long, J., Wan, Y., Luo, F., Zhao, X., Qian, Z., 2011. Curcumin-loaded biodegradable polymeric micelles for colon cancer therapy *in vitro* and *in vivo*. Nanoscale, 3(4), 1558-1567. doi: 10.1039/c0nr00758g.

Guan, Y-B., Zhou, S-Y., Zhang, Y-Q., Wang, J.-l., Tian, Y-D., Jia, Y-Y., Sun, Y-J., 2017. Therapeutic effects of curcumin nanoemulsions on prostate cancer. J Huazhong Univ Sci Technolog Med Sci. 37(3), 371-378. doi: 10.1007/s11596-017-1742-8.

Guerrero, S., Inostroza-Riquelme, M., Contreras-Orellana, P., Diaz-Garcia, V., Lara, P., Vivanco-Palma, A., Cárdenas, A., Miranda, V., Robert, P., Leyton, L., Kogan, M.J., Quest, A.F.G., Oyarzun-Ampuero, F., 2018. Curcumin-loaded nanoemulsion: a new safe and effective formulation to prevent tumor reincidence and metastasis. Nanoscale 10:22612-22622. doi: 10.1039/c8nr06173d.

Guo, Q., Bayram, I., Zhang, W., Su, J., Shu, X., Yuan, F., Mao, L., Gao, Y., 2021. Fabrication and characterization of curcumin-loaded pea protein isolate-surfactant complexes at neutral pH. Food Hydrocolloid, 111, 106214. doi: https://doi.org/10.1016/j.foodhyd.2020.106214.

Gupta, S.C., Prasad, S., Kim, J.H., Patchva, S., Webb, L.J., Priyadarsini, I.K., Aggarwal, B.B., 2011. Multitargeting by curcumin as revealed by molecular interaction studies. Nat Prod Rep. 28(12), 1937-1955. doi: 10.1039/c1np00051a.

Gupta, S.C., Kismali, G, Aggarwal, B. B., 2013. Curcumin, a component of turmeric: from farm to pharmacy. Biofactors. 39(1), 2-13. doi: 10.1002/biof.1079.

Heffernan, C., Ukrainczyk, M., Gamidi, R.K., Hodnett, B.K., Rasmuson, Å.C., 2017. Extraction and purification of curcuminoids from crude curcumin by a combination of crystallization and chromatography. Org Process Res Dev. 21, 821−826. doi: 10.1021/acs.oprd.6b00347.

Jiang, T., Liao, W., Charcosset, C., 2020. Recent advances in encapsulation of curcumin in nanoemulsions: A review of encapsulation technologies, bioaccessibility and applications. Food Res Int. 132, 109035. doi: 10.1016/j.foodres.2020.109035.

Jiao, D., Wang, J., Lu, W., Tang, X., Chen, J., Mou, H., Chen, Q-Y., 2016. Curcumin inhibited HGF-induced EMT and angiogenesis through regulating c-Met dependent PI3K/Akt/mTOR signaling pathways in lung cancer. Mol Ther Oncolytics. 3, 16018-16018. doi: 10.1038/mto.2016.18.

Jose, A., Labala, S., Ninave, K.M., Gade, S.K., Venuganti, V.V.K., 2018. Effective skin cancer treatment by topical co-delivery of curcumin and STAT3 siRNA using cationic liposomes. AAPS PharmSciTech. 19(1), 166-175. doi: 10.1208/s12249-017-0833-y.

Khaw, A.K., Hande, M.P., Kalthur, G., Hande, M.P., 2013. Curcumin inhibits telomerase and induces telomere shortening and apoptosis in brain tumour cells. J Cell Biochem. 114(6), 1257-70. doi: 10.1002/jcb.24466.

Kim, H., Park, J., Tak, K.-H., Bu, S. Y., Kim, E., 2014. Chemopreventive effects of curcumin on chemically induced mouse skin carcinogenesis in BK5.insulin-like growth factor-1 transgenic mice. *In Vitro* Cell Dev Biol Anim. 50(9), 883-92. doi: 10.1007/s11626-014-9791-9.

Kotha, R.R., Luthria, D.L., 2019. Curcumin: Biological, pharmaceutical, nutraceutical, and analytical aspects. Molecules. 24(16), 2930. doi:10.3390/molecules24162930.

Kumari, P., Muddineti, O.S., Rompicharla, S.V.K., Ghanta, P., Adithya Karthik, B. B. N., Ghosh B., Biswas, S., 2017. Cholesterol-conjugated poly(D, L-lactide)-based micelles as a nanocarrier system for effective delivery of curcumin in cancer therapy. Drug Delivery. 24:1, 209-223. doi: 10.1080/10717544.2016.1245365.

Kurnik, I.S., Noronha, M.A., Câmara, M.C., Mazzola, P.G., Vicente, A.A., Pereira, J.F., Lopes, A.M., 2020. Separation and purification of curcumin using novel aqueous two-phase micellar systems composed of amphiphilic copolymer and cholinium ionic liquids. Sep Purif Technol. 250(1), 117262. doi: 10.1016/j.seppur.2020.117262.

Kurnik, I.S, D'Angelo, N., Mazzola, P.G., Chorilli, M., Kamei, D., Pereira, J.F., Vicente, A.A. Lopes, A. 2021. Polymeric micelles using cholinium-based ionic liquids for the encapsulation and drug release of hydrophobic molecules. Biomaterials Science. doi: https://doi.org/10.1039/D0BM01884H.

Kuttan, R., Bhanumathy, P., Nirmala, K., George, M.C., 1985 Potential anticancer activity of turmeric (*Curcuma longa*). Cancer lett. 29(2), 197-202. doi: 10.1016/0304-3835(85)90159-4.

Lachowicz, D., Karabsz, A., Bzowska, M., Szuwarzynski, M., Karewicz, A., Nowakowska, M., 2019. Blood-compatible, stable micelles of sodium alginate – Curcumin bioconjugate for anti-cancer applications. Euro Pol J. 113, 208-219. 10.1016/j.eurpolymj.2019.01.058.

Lee, W., Lee, D.G., 2014. An antifungal mechanism of curcumin lies in membrane-targeted action within *Candida albicans*. IUBMB Life. 66(11), 780-785. doi: 10.1002/iub.1326.

Lelli, D., Pedone, C., Sahebkar, A., 2017 Curcumin and treatment of melanoma: The potential role of microRNAs. Biomed Pharmacother. 88, 832-834. doi: 10.1016/j.biopha.2017.01.078.

Lestari, B., Nakame, I., Yoneda-Kato, N., Morimoto, T., Kanaya, S., Yokoyama, T., Shionyo, M., Shirai, T., Meiyanto, E., Kato, J.-Y., 2019. Pentagamavunon-1 (PGV-1) inhibits ROS metabolic enzymes and suppresses tumor cell growth by inducing M phase (prometaphase) arrest and cell senescence. Sci Rep. 16;9(1), 14867. doi: 10.1038/s41598-019-51244-3.

Leung, M.H.M., Kee, T.W., 2009. Effective stabilization of curcumin by association to plasma proteins: human serum albumin and fibrinogen. Langmuir. 25(10), 5773-7. doi: 10.1021/la804215v.

Li, L., Xiang, D., Shigdar, S., Yang, W., Li, Q., Lin, J., Liu, K., Duan, W., 2014. Epithelial cell adhesion molecule aptamer functionalized PLGA-Lecithin-Curcumin-PEG nanoparticles for targeted drug delivery to human colorectal adenocarcinoma cells. Int. J. Nanomedicine. 9, 1083-1096. doi: 10.2147/IJN.S59779.

Li, R., Lin, Z., Zhang, Q., Zhang, Y., Liu, Y., Lyu, Y., 2020. Injectable and *in-situ* formable thiolated chitosan coated liposomal hydrogels as curcumin carriers for prevention of *in vivo* breast cancer recurrence. ACS Appl Mater Interfaces. 12(15), 17936-17948. doi: 10.1021/acsami.9b21528.

Liu, F., Ma, D., Luo, X., Zhang, Z., He, L., Gao, Y., McClements, D.J., 2018. Fabrication and characterization of protein-phenolic conjugate nanoparticles for co-delivery of curcumin and resveratrol. Food Hydrocolloid, 79, 450-461. doi: https://doi.org/10.1016/j.foodhyd.2018.01.017.

Liu, W.-L., Chang, J.-M., Chong, I.-W., Hung, Y.-L., Chen, Y.-H., Huang, W.-T., Kuo, H.-F., Hsieh, C.-C., Liu, P.-L., 2017. Curcumin inhibits LIN-28A through the activation of miRNA-98 in the lung cancer cell line A549. Molecules. 22(6),929. doi: 10.3390/molecules22060929.

Liu, Z., Liu, C., Sun, X., Zhang, S., Yuan, Y., Wang, D., Xu, Y., 2020. Fabrication and characterization of cold-gelation whey protein-chitosan complex hydrogels

for the controlled release of curcumin. Food Hydrocolloid, 103, 105619. doi: https://doi.org/10.1016/j.foodhyd.2019.105619.

Luong, D., Kesharwani, P., Alsaab, H.O., Sau, S., Padhye, S., Sarkar, F.H., Iyer, A.K., 2017. Folic acid conjugated polymeric micelles loaded with a curcumin difluorinated analog for targeting cervical and ovarian cancers. Colloids Surf B Biointerfaces. 157, 490-502. doi: 10.1016/j.colsurfb.2017.06.025.

Ma, Q., Qian, W., Tao, W., Zhou, Y., Xue, B., 2019. Delivery of curcumin nanoliposomes using surface modified with CD133 aptamers for prostate cancer. Drug Des Devel Ther. 13, 4021–33. doi: 10.2147/DDDT.S210949.

Machado, F.C., Adum de Matos, R.P., Primo, F.L., Tedesco, A.C., Rahal, P., Calmon, M.F., 2019. Effect of curcumin-nanoemulsion associated with photodynamic therapy in breast adenocarcinoma cell line. Bioorg Med Chem. 27, 1882-1890. doi: 10.1016/j.bmc.2019.03.044.

Mahmoud, D.B.E.D., Marzok, S., 2020. In situ supersaturable polyhydrogels: A feasible modification of the conventional hydrogels for the enhanced delivery of stomach specific hydrophobic drugs. J Drug Deliv Sci Technol. 58, 101744. doi: 10.1016/j.jddst.2020.101744.

Mandal, S., Banerjee, C., Ghosh, S., Kuchlyan, J., Sarkar, N., 2013. Modulation of the photophysical properties of curcumin in nonionic surfactant (Tween-20) forming micelles and niosomes: a comparative study of different microenvironments. J Physical Chem B. 117, 6957−6968. doi: 10.1021/jp403724g.

Mangolim, C.S., Moriwaki, C., Nogueira, A.C., Sato, F., Baesso, M.L., Neto, A.M., Matioli, G., 2014. Curcumin–β-cyclodextrin inclusion complex: Stability, solubility, characterisation by FT-IR, FT-Raman, X-ray diffraction and photoacoustic spectroscopy, and food application. Food Chemistry 153, 361–370. doi: 10.1016/j.foodchem.2013.12.067.

Martínez-Guerra, J., Palomar-Pardavé, M., Romero-Romo, M., Corona-Avendaño, S., Rojas-Hernández, A., Ramírez-Silva, M.T., 2019. New insights on the chemical stability of curcumin in aqueous media at different ph: influence of the experimental conditions. Int. J. Electrochem. Sci., 14, 5373 – 5385. doi: 10.20964/2019.06.24.

Mathew, D., Hsu, W.L., 2018. Antiviral potential of curcumin. J. Func. Foods. 40, 692-699. doi:10.1016/j.jff.2017.12.017.

McClements D.J., Rao J., 2011. Food-Grade Nanoemulsions: Formulation, Fabrication, Properties, Performance, Biological Fate, and Potential Toxicity. Crit Rev Food Sci Nutr. 51, 285-330. doi: 10.1080/10408398.2011.559558.

Mirzaee, F., Hosseinzadeh, L., Ashrafi-Kooshk, M.R., Esmaeili, S., Ghobadi, S., Farzaei , M.H., Zad-Bari, M.R., Khodarahmi, R., 2019. Diverse effects of different "protein-based" vehicles on the stability and bioavailability of curcumin:

spectroscopic evaluation of the antioxidant activity and cytotoxicity *in vitro*. Protein Pept Lett. 26(2), 132-147. doi: 10.2174/0929866525666181114152242.

Moghadamtousi, S.Z., Kadir, H.A., Hassandarvish, P., Tajik, H., Abubakar, S., Zandi, K., 2014. A review on antibacterial, antiviral, and antifungal activity of curcumin. Biomed Res Int. 2014:186864. doi: 10.1155/2014/186864.

Moghaddasi, F., Housaindokht, M.R., Darroudi, M., Bozorgmehr, M.R., Sadeghi, A., 2018. Synthesis of nano curcumin using black pepper oil by O/W Nanoemulsion Technique and investigation of their biological activities. Lwt. 92, 92-100. doi: 10.1016/j.lwt.2018.02.023.

Moghassemi, S., Hadjizadeh, A., 2014. Nano-niosomes as nanoscale drug delivery systems: An illustrated review. J Controll Release. 185, 22-36. doi: 10.1016/j.jconrel.2014.04.015.

Momoh, M.A., Esimone, C.O., 2012. Phospholipon 90H (P90H)-Based PEGylated microscopic liposphere delivery system for gentamicin: An antibiotic evaluation. Asian Pac J Trop Biomed. 2(11), 889–94. doi: 10.1016/S2221-1691(12)60248-2.

Mounce, B.C., Cesaro, T., Carrau, L., Vallet, T., Vignuzzi, M., 2017. Curcumin inhibits Zika and chikungunya virus infection by inhibiting cell binding. Antiviral Res. 142, 148-157. doi: 10.1016/j.antiviral.2017.03.014.

Naksuriya, O., Okonogi, S., Schiffelers, R. M., Hennink, W. E., 2014. Curcumin nanoformulations: a review of pharmaceutical properties and preclinical studies and clinical data related to cancer treatment. Biomaterials, 35(10), 3365-3383.

Neelofar, K., Shreaz, S., Rimple, B., Muralidhar, S., Nikhat, M., Khan, L.A., 2011. Curcumin as a promising anticandidal of clinical interest. Can J Microbiol. 57,204-210. doi:10.1139/w10-117.

Nikolic I., Mitsou E., Damjanovic A., Papadimitriou V., Antic-Stankovic J., Stanojevic B., Xenakis A., Savic S., 2020. Curcumin-loaded low-energy nanoemulsions: Linking EPR spectroscopy-analysed microstructure and antioxidant potential with *in vitro* evaluated biological activity. J Mol Liq. 301, 112479. doi: 10.1016/j.molliq.2020.112479.

Ning, P., Lü, S., Bai, X., Wu, X., Gao, C., Wen, N., Liu, M., 2018. High encapsulation and localized delivery of curcumin from an injectable hydrogel. Mater Sci Eng C Mater Biol Appl. 83, 121-129. doi: 10.1016/j.msec.2017.11.022.

Ntoutoume, G.M.N., Granet, R., Mbakidi, J.P., Brégier, F., Léger, D.Y., Fidanzi-Dugas, C., Lequart, V., Joly, N., Liagre, B., Chaleix, V., Sol, V., 2016. Development of curcumin–cyclodextrin/cellulose nanocrystals complexes: New anticancer drug delivery systems. Bioorg Med Chem Lett. 26(3):941-945. doi: 10.1016/j.bmcl.2015.12.060.

Olotu, F., Agoni, C., Soremekun, O., Soliman, M.E.S., 2020. An update on the pharmacological usage of curcumin: has it failed in the drug discovery pipeline? Cell Biochem Biophys. 78(3), 267-289. doi: 10.1007/s12013-020-00922-5.

Olszewska, M.A., Gędas, A., Simões, M., 2020. Antimicrobial polyphenol-rich extracts: Applications and limitations in the food industry. Food Res Int. 134,109214. doi: 10.1016/j.foodres.2020.109214.

Patel, S.S., Acharya, A., Ray, R.S., Agrawal, R., Raghuwanshi, R., Jain, P., 2020. Cellular and molecular mechanisms of curcumin in prevention and treatment of disease. Crit Rev Food Sci Nutr. 60(6), 887-939. doi: 10.1080/10408398.2018.1552244.

Patil, S.S., Bhasarkar, S., Rathod, V.K., 2019. Extraction of curcuminoids from *Curcuma longa*: comparative study between batch extraction and novel three phase partitioning. Prep. Biochem. Biotechnol. 49(4), 407−418. doi: 10.1080/10826068.2019.1575859.

Pettinelli, N., Rodríguez-Llamazares, S., Bouza, R., Barral, L., Feijoo-Bandínde, S., Lago, F., 2020. Carrageenan-based physically crosslinked injectable hydrogel for wound healing and tissue repairing applications. Int J Pharm. 589, 119828. doi: 10.1016/j.ijpharm.2020.119828.

Pinheiro, A.C., Coimbra, M.A., Vicente, A.A., 2016. *In vitro* behaviour of curcumin nanoemulsions stabilized by biopolymer emulsifiers – Effect of interfacial composition. Food Hydrocoll. 52, 460-467. doi: 10.1016/j.foodhyd.2015.07.025.

Prasad, S., Aggarwal, B.B., 2011. Turmeric the Golden Spice: From Traditional Medicine to Modern Medicine. In: Benzie IFF, Wachtel-Galor S. (EDS), Herbal Medicine: Biomolecular and Clinical Aspects. 2nd ed. CRC Press/Taylor & Francis, Boca Raton (FL), 13.

PubChem. https://pubchem.ncbi.nlm.nih.gov/compound/969516#section=Chemical-and-Physical-Properties (accessed 18 July 2020).

Pushpalatha, R., Selvamuthukumar, S., Kilimozhi, D., 2019. Cyclodextrin nanosponge based hydrogel for the transdermal co-delivery of curcumin and resveratrol: Development, optimization, *in vitro* and *ex vivo* evaluation. J Drug Deliv Sci Technol. 52, 55-64. doi: 10.1016/j.jddst.2019.04.025.

Puvvada, N., Rajput, S., Kumar, B.N.P., Mandalb, M., Pathal, A., 2013. Exploring the fluorescence switching phenomenon of curcumin encapsulated niosomes: *in vitro* real time monitoring of curcumin release to cancer cells. RSC Advances. 3(8), 2553. doi: 10.1039/c2ra23382g.

Rafiee Z., Nejatian M., Daeihamed M., Jafari S.M., 2018. Application of different nanocarriers for encapsulation of curcumin. Crit Rev Food Sci Nutr. 59, 3468-3497. doi: 10.1080/10408398.2018.1495174.

Riaz, M.K., Riaz, M.A., Zhang, X., Lin, C., Wong, K.H., Chen, X., Zhang, G., Lu, A., Yang, Z., 2019. Surface functionalization and targeting strategies of liposomes in solid tumor therapy: A review. Int J Mol Sci. 19(1). doi: 10.3390/ijms19010195.

Rocks, N., Bekaert, S., Coia, I., Paulissen, G., Gueders, M., Evrard, B., Van Heugen, J-C., Chiap, P., Foidart, J-M ., Noel, A., Cataldo, D., 2012. Curcumin–cyclodextrin complexes potentiate gemcitabine effects in an orthotopic mouse model of lung cancer. Br J Cancer. 107, 1083–1092. doi: 10.1038/bjc.2012.379.

Ruttala, H.B., Ko, Y.T., 2015. Liposomal co-delivery of curcumin and albumin/paclitaxel nanoparticle for enhanced synergistic antitumor efficacy. Coll Surf B Bio. 128, 419–26. doi: 10.1016/j.colsurfb.2015.02.040.

Saengkrit, N., Saesoo, S., Srinuanchai, W., Phunpee, S., Ruktanonchai, U.R., 2014. Influence of curcumin-loaded cationic liposome on anticancer activity for cervical cancer therapy. Coll Surf B Bio. 114, 349–56. doi: 10.1016/j.colsurfb.2013.10.005.

Salem, M., Rohani, S., Gillies, E.R., 2014. Curcumin, a promising anti-cancer therapeutic: a review of its chemical properties, bioactivity and approaches to cancer cell delivery. RSC advances. 4(21), 10815-10829. doi: 10.1039/C3RA46396F

Salvia-Trujillo, L., Soliva-Fortuny, R., Rojas-Graü, M.A., McClements, D.J., Martín-Belloso, O., 2017. Edible nanoemulsions as carriers of active ingredients: a review. Annu Rev Food Sci Technol. 8:439-466. doi: 10.1146/annurev-food-030216-025908.

Sari, T.P., Mann, B., Kumar, R., Singh, R.R.B., Sharma, R., Bhardwaj, M., Athira, S., 2015. Preparation and characterization of nanoemulsion encapsulating curcumin. Food Hydrocol. 43, 540-546. doi: 10.1016/j.foodhyd.2014.07.011.

Sarika, P.R., James, N.R., Kumar, A., Raj, D., 2016. Galactosylated alginate-curcumin micelles for enhanced delivery of curcumin to hepatocytes Int J Biol Macromol. 86,1-9. doi: 10.1016/j.ijbiomac.2016.01.037.

Schneider, C., Gordon, O.N., Edwards, R.L., Luis, P.B., 2015. Degradation of curcumin: from mechanism to biological implications. J Agric Food Chem. 63, 7606–7614. doi: 10.1021/acs.jafc.5b00244.

Seleci, D.A., Seleci, M., Stahl, F., Scheper, T., 2017. Tumor homing and penetrating peptide-conjugated niosomes as multi-drug carriers for tumor-targeted drug delivery. RSC Advances. (7)53, 33378-33384. doi: 10.1039/c7ra05071b.

Sercombe, L., Veerati, T., Moheimani, F., Wu, S.Y., Sood, A.K., Hua, S., 2015. Advances and challenges of liposome assisted drug delivery. Front Pharmacol. 6, 1–13. doi: 10.3389/fphar.2015.00286.

Sesarman, A., Tefas, L., Sylvester, B., Licarete, E., Rauca, V., Luput, L., Patras, L., Porav, S., Banciu, M., Porfire, A., 2019. Co-delivery of curcumin and doxorubicin in PEGylated liposomes favored the antineoplastic C26 murine colon carcinoma microenvironment. Drug Deliv Transl Res. 9(1), 260–72. doi: 10.1007/s13346-018-00598-8.

Sharma, M., Manoharlal, R., Puri, N., Prasad, R., 2010. Antifungal curcumin induces reactive oxygen species and triggers an early apoptosis but prevents hyphae development by targeting the global repressor TUP1 in *Candida albicans*. Bio Reports. 30, 391-404. doi:10.1042/bsr20090151.

Sharma, V., Anandhakumar, S., Sasidharan, M., 2015. Self-degrading niosomes for encapsulation of hydrophilic and hydrophobic drugs: An efficient carrier for cancer multi-drug delivery. Mater Sci Eng C. 56, 393-400. doi: 10.1016/j.msec.2015.06.049.

Shehzad, A., Lee, J., Lee, Y.S., 2013a. Curcumin in various cancers. Biofactors. 39(1), 56-68. doi: 10.1002/biof.1068.

Shehzad, A., Lee, Y.S., 2013b. Molecular mechanisms of curcumin action: signal transduction. Biofactors. 39(1), 27-36. doi: 10.1002/biof.1065.

Shukla, M., Jaiswal, S., Sharma, A., Srivastava, P.K., Arya, A., Dwivedi, A.K., Lal, J., 2017. A combination of complexation and self-nanoemulsifying drug delivery system for enhancing oral bioavailability and anticancer efficacy of curcumin. Drug Dev Ind Pharm. 43(5), 847-861. doi: 10.1080/03639045.2016.1239732.

Singh, M., Singh, N., 2011. Curcumin counteracts the proliferative effect of estradiol and induces apoptosis in cervical cancer cells. Mol Cell Biochem 347, 1–11. doi: 10.1007/s11010-010-0606-3.

Singh, R., Tønnesen, H.H., Vogensen, S.B., Loftsson, T., Másson, M., 2010. Studies of curcumin and curcuminoids. The stoichiometry and complexation constants of cyclodextrin complexes as determined by the phase-solubility method and UV–Vis titration. J Incl Phenom Macrocycl Chem. 66, 335–348. doi: 10.1007/s10847-009-9651-5.

Sintov, A.C., 2015. Transdermal delivery of curcumin via microemulsion. .Int J Pharm. 481(1-2):97-103. doi: 10.1016/j.ijpharm.2015.02.005.

Sneharani, A.H., Karakkat, J.V., Singh, S.A., Rao, A.G.A., 2010. Interaction of curcumin with β-lactoglobulin-stability, spectroscopic analysis, and molecular modeling of the complex. J. Agric. Food Chem. 58, 11130–11139. doi: 10.1021/jf102826q.

Sneharani, A.H., Singh, S.A., Appu Rao, A.G., 2009. Interaction of αS1-casein with curcumin and its biological implications. J. Agric. Food. Chem. 57(21), 10386-91. doi: https://doi.org/10.1021/jf902464p.

Songkroh, T., Xiel, H., Yu, W., Liu, X., Sun, G., Xu, X., Ma, X., 2015. Injectable *in situ* forming chitosan-based hydrogels for curcumin delivery. Macromolecular Research, 23, 1, 53-59. doi: 10.1007/s13233-015-3006-4.

Stohs, S.J.; Chen, O.; Ray, S.D.; Ji, J., Bucci, L.R.; Preuss, H.G., 2020. Highly bioavailable forms of curcumin and promising avenues for curcumin-based research and application: A review. Molecules, 25(6), 1397. Doi: https://doi.org/10.3390/molecules25061397.

Sun, D., Zhou, J.K., Zhao, L., Zheng, Z.Y., Li, J., Pu, W., 2017. Novel curcumin liposome modified with hyaluronan targeting CD44 plays an anti-leukemic role in acute myeloid leukemia *in vitro* and *in vivo*. ACS Appl Mater Interfaces. 9(20):16857-16868. doi: 10.1021/acsami.7b02863.

Sun, Y., Du, L., Liu, Y., Li, X., Li, M., Jin, Y., Qian, X., 2014. Transdermal delivery of the in situ hydrogels of curcumin and its inclusion complexes of hydroxypropyl-β-cyclodextrin for melanoma treatment. Int J Pharm. 469(1):31-9. doi: 10.1016/j.ijpharm.2014.04.039.

Tian, B., Zhao, Y., Liang, T., Ye, X., Li, Z., Yan, D., Fu, Q., Li, Y., 2017. Curcumin inhibits urothelial tumor development by suppressing IGF2 and IGF2-mediated PI3K/AKT/mTOR signaling pathway. J Drug Target. 25(7), 626-636. doi: 10.1080/1061186X.2017.1306535.

Tian, C., Asghar, S., Xu, Y., Chen, Z., Zhang, J., Ping, Q., Xiao, Y., 2018. Tween 80-modified hyaluronic acid-ss-curcumin micelles for targeting glioma: Synthesis, characterization and their *in vitro* evaluation. Int J Biol Macromol. 120(Pt B), 2579-2588. doi: 10.1016/j.ijbiomac.2018.09.034.

Tima, S., Anuchapreeda, S., Ampasavate, C., Berkland, C., Okonogi, S., 2017. Stable curcumin-loaded polymeric micellar formulation for enhancing cellular uptake and cytotoxicity to FLT3 overexpressing EoL-1 leukemic cells. Eur. J. Pharm. Biopharm.. 114, 57-68. doi: 10.1016/j.ejpb.2016.12.032.

Tyagi, P., Singh, M., Kumari, H., Kumari, A., Mukhopadhyay, K., 2015. Bactericidal activity of curcumin I is associated with damaging of bacterial membrane. PLoS One. 10(3), e0121313. doi: 10.1371/journal.pone.0121313.

Ukrainczyk, M., Hodnett, B.K., Rasmuson, Å.C., 2016. Process parameters in the purification of curcumin by cooling crystallization, Org. Process Res. Dev. 20, 1593−1602. doi: 10.1021/acs.oprd.6b00153.

van Hoogevest, P., 2017. Review – An update on the use of oral phospholipid excipients, Eur J Pharm Sci. 108, 1–12. doi: http://dx.doi.org/10.1016/j.ejps.2017.07.008.

Vijayan, U.K., Shah, N.N., Muley, A.B., Singhal, R.S., 2021. Complexation of curcumin using proteins to enhance aqueous solubility and bioaccessibility: Pea protein vis-à-vis whey protein. J Food Eng. 292, 110258. doi: https://doi.org/10.1016/j.jfoodeng.2020.110258.

Wan, K., Sun, L., Hu, X., Yan, Z., Zhang, Y., Zhang, X., Zhang, J., 2016. Novel nanoemulsion based lipid nanosystems for favorable *in vitro* and *in vivo* characteristics of curcumin. Int J Pharm. 504, 80-88. doi: 10.1016/j.ijpharm.2016.03.055.

Wang, B., He, X., Zhang, Z., Zhao, Y., Feng, W., 2013. Metabolism of nanomaterials *in vivo*: blood circulation and organ clearance, Accounts Chem Res, 46(3), 761-769. doi: https://doi.org/10.1021/ar2003336.

Wang, X., Huang, H., Chu, X., Han, Y., Li, M., Li, G., Liu, X., 2019. Encapsulation and binding properties of curcumin in zein particles stabilized by Tween 20. Colloid Surface A. 577, 274-280. doi: https://doi.org/10.1016/j.colsurfa.2019.05.094.

Wang, Y., Yu, J., Cui, R., Lin, J., Ding, X., 2016. Curcumin in treating breast cancer: a review. J Lab Autom. 21(6), 723-731. doi: 10.1177/2211068216655524.

Wichterle, O., Lím, D., 1960. Hydrophilic gels for biological use. Nature, 185, 117–118. doi: https://doi.org/10.1038/185117a0.

Winter, S., Tortik, N., Kubin, A., Krammer, B., Plaetzer, K., 2013. Back to the roots: photodynamic inactivation of bacteria based on water-soluble curcumin bound to polyvinylpyrrolidone as a photosensitizer Photochem Photobiol Sci. 12(10), doi: 10.1039/c3pp50095k.

Wu, J., Lu, W.-Y., Cui, L.-L., 2015. Inhibitory effect of curcumin on invasion of skin squamous cell carcinoma A431 cells. Asian Pac J Cancer Prev. 16(7), 2813-8. doi: 10.7314/apjcp.2015.16.7.2813.

Xu, H., Gong, Z., Zhou, S., Yang, S., Wang, D., Chen, X., Wu, J., Liu, L., Zhong, S., Zhao, J., Tang, J., 2018. Liposomal curcumin targeting endometrial cancer through the NF-κB pathway. Cell Physiol Biochem. 48(2):569-582. doi: 10.1159/000491886.

Xu, Y.Q., Chen, W.R., Tsosie, J.K., Xie, X., Li, P., Wan, J.B., He, C.W., Chen, M.W., 2016. Niosome encapsulation of curcumin: characterization and cytotoxic effect on ovarian cancer cells. J Nanomaterials. 1-9, doi: 10.1155/2016/6365295.

Yadav, V.R., Suresh, S., Devi, K., Yadav, S., 2009. Effect of cyclodextrin complexation of curcumin on its solubility and antiangiogenic and anti-inflammatory activity in rat colitis model. AAPS PharmSciTech. 10, 752. doi: 10.1208/s12249-009-9264-8.

Yallapu, M.M., Jaggi, M., Chauhan, S.C., 2010. Poly(β-cyclodextrin)/curcumin self-assembly: a novel approach to improve curcumin delivery and its therapeutic efficacy in prostate cancer cells. Macromol Biosci. 10(10):1141-51. doi: 10.1002/mabi.201000084.

Yallapu, M.M., Jaggi, M., Chauhan, S.C., 2012. Curcumin nanoformulations: a future nanomedicine for cancer. Drug Discov Today. 17(1-2):71-80. doi:10.1016/j.drudis.2011.09.009.

Yang, M., Wu, Y., Li, J., Zhou, H., Wang, X., 2013. Binding of curcumin with bovine serum albumin in the presence of ι-carrageenan and implications on the stability and antioxidant activity of curcumin. J. Agric. Food Chem. 61, 7150–7155. doi: 10.1021/jf401827x.

Yi, J., Fan, Y., Zhang, Y., Wen, Z., Zhao, L., Lu, Y., 2016. Glycosylated α-lactalbumin-based nanocomplex for curcumin: Physicochemical stability and DPPH-scavenging activity. Food Hydrocoll. 61, 369–377. doi: 10.1016/j.foodhyd.2016.05.036.

Yoon, H.J., Zhang, X., Kang, M.G., Kim, G.J., Shin, S.Y., Baek, S.H., Lee, B.N., Hong, S.J., Kim, J.T., Hong, K., Bae, H., 2018. Cytotoxicity evaluation of turmeric extract incorporated oil-in-water nanoemulsion. Int J Mol Sci. 19(1), 280. doi: 10.3390/ijms19010280.

Zaman, H., Bright, A.G., Adams, K., Goodall, D.M., Forbes, R.T., 2017. Characterization of aggregates of cyclodextrin-drug complexes using Taylor Dispersion Analysis. Int J Pharm. 522, 98–109. doi: 10.1016/j.ijpharm.2017.02.012.

Zhang, C.-Y., Zhang, L., Yu, H.-X., Bao, J.-D., Sun, Z., Lu, R.-R., 2013. Curcumin inhibits invasion and metastasis in K1 papillary thyroid cancer cells. Food Chem. 139(1-4), 1021-8. doi: 10.1016/j.foodchem.2013.02.016.

Zhang, D., Xu, Q., Wang, N., Yang, Y., Liu, J., Yu, G., Yang, X., Xu, H., Wang, H., 2018a. A complex micellar system co-delivering curcumin with doxorubicin against cardiotoxicity and tumor growth. Int J Nanomedicine. 10(13), 4549-4561. doi: 10.2147/IJN.S170067.

Zhang, L., Man, S., Qiu, H., Liu, Z., Zhang, M., Ma, L., Gao, W., 2016. Curcumin-cyclodextrin complexes enhanced the anti-cancer effects of curcumin. Environ Toxicol Pharmacol. 48, 31-38. doi: 10.1016/j.etap.2016.09.021.

Zhang, T., Chen, Y., Ge, Y., Hu, Y., Li, M., Jin, Y., 2018b. Inhalation treatment of primary lung cancer using liposomal curcumin dry powder inhalers. Acta Pharm Sin B. 8(3), 440–8. doi: 10.1016/j.apsb.2018.03.004.

Zhao, G., Sun, Y., Dong, X., 2020. Zwitterionic polymer micelles with dual conjugation of doxorubicin and curcumin: synergistically enhanced efficacy against multidrug-resistant tumor cells. Langmuir. 36, 2383-2395. doi: 10.1021/acs.langmuir.9b03722.

Zheng, S., Gao, X., Liu, X., Yu, T., Zheng, T., Wang, Y., You, C., 2016. Biodegradable micelles enhance the antiglioma activity of curcumin *in vitro* and *in vivo*. Int J Nanomedicine. 11, 2721-36. doi: 10.2147/IJN.S102450.

Zhu, G.-H., Dai, H.-P., Shen, Q., Ji, O., Zhang, Q., Zhai, Y.-L., 2016 Curcumin induces apoptosis and suppresses invasion through MAPK and MMP signaling in human monocytic leukemia SHI-1 cells. Pharm Biol. 54(8), 1303-11. doi: 10.3109/13880209.2015.1060508.

Zhu, J.-Y., Yang, X., Chen, Y., Jiang, Y., Wang, S.-J., Li, Y., Wang, X.-Q., Meng, Y., Zhu, M.-M., Ma, X., Huang, C., Wu, R., Xie, C.-F., Li, X.-T., Geng, S.-S., Wu, J.-S., Zhong, C.-Y., Han, H.-Y., 2017. Curcumin suppresses lung cancer stem cells via inhibiting Wnt/β-catenin and sonic hedgehog pathways. Phytother Res. 31(4), 680-688. doi: 10.1002/ptr.5791.

Zielińska, A., Alves, H., Marques, V., Durazzo, A., Lucarini, M., Alves, T. F., Morsink, M., Willemen, N., Eder, P., Chaud, M.V., Severino, P., Santini, A., Souto, E.B., 2020a. Properties, extraction methods, and delivery systems for curcumin as a natural source of beneficial health effects. Medicina (Kaunas). 56(7), 336. doi: 10.3390/medicina56070336.

Zielińska, A., Costa, B., Ferreira, M. V., Miguéis, D., Louros, J., Durazzo, A., Willemen, N., 2020b. Nanotoxicology and nanosafety: safety-by-design and testing at a glance. Int J Environ Res Public Health. 17(13), 4657. doi: 10.3390/ijerph17134657.

Conflict of Interest

The authors declare that they have no known competing financial interests or personal relationships that could have appeared to influence the work reported in this paper.

CRediT authorship contribution statement

Natália A. D'Angelo, Mariana A. Noronha, Isabelle S. Kurnik, Mayra C. C. Câmara, Jorge Vieira, Luís Abrunhosa, Joana T. Martins, Thais F. R. Alves, Louise L. Tundisi, Janaina A. Ataide, and Juliana S. R. Costa: Writing-Original draft preparation, Literature reviewing, Manuscript writing. **Angela F. Jozala, Laura O. Nascimento, Priscila G. Mazzola, Marco V. Chaud, and António A. Vicente:** Writing-Reviewing and Editing. **Andre M. Lopes:** Conceptualization, Writing - review & editing, Supervision.